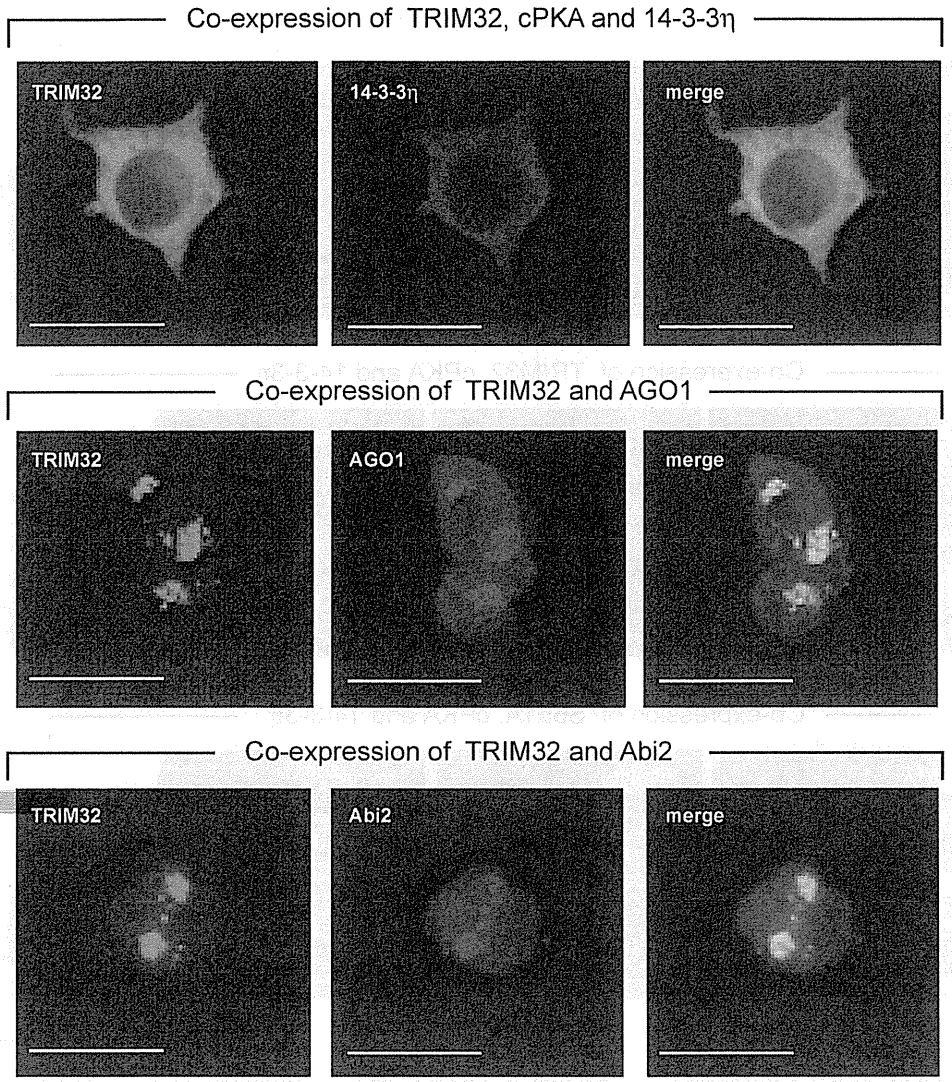


**Fig. S2. Coexpression of 14-3-3η, but not AGO1 and Abi2, suppresses the formation of TRIM32 CBs.** HEK293 cells were co-transfected with the indicated constructs (myc-TRIM32, FLAG-14-3-3η, FLAG-AGO1, FLAG-Abi2, cPKA), and after 24 h the cells were stained with monoclonal mouse anti-myc (green) and polyclonal rabbit anti-FLAG (red). Note that coexpression of 14-3-3η, but not AGO1 and ABi2, specifically disperses the TRIM32 protein throughout the cytoplasm. Scale bars: 10 μm.

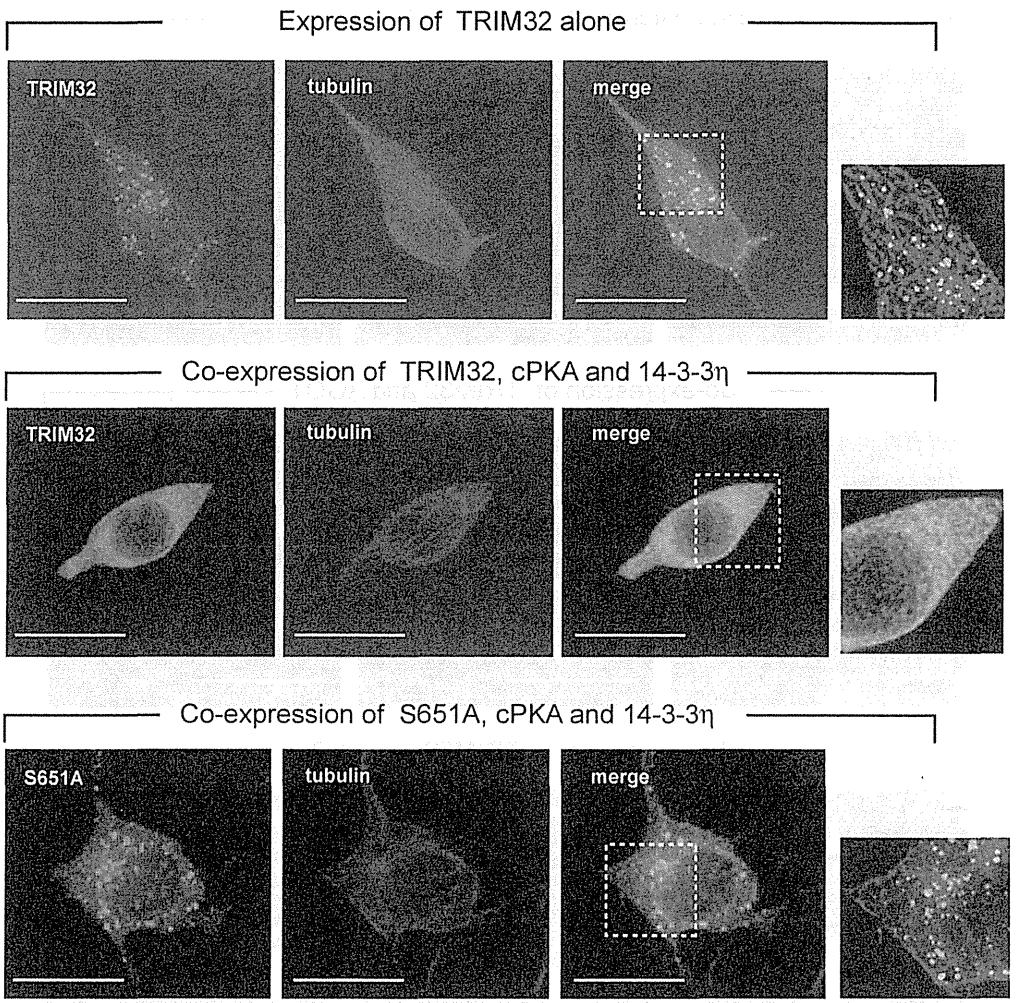


**Fig. S3. Coexpression of 14-3-3η suppresses the association of TRIM32 with microtubules.** HEK293 cells were co-transfected with the indicated constructs (FLAG-TRIM32, FLAG-S651A, myc-14-3-3η, cPKA), and after 12–16 h the cells were stained with polyclonal anti-FLAG-TRIM32 (green) and monoclonal anti-α-tubulin (red). Scale bars: 10 μm.

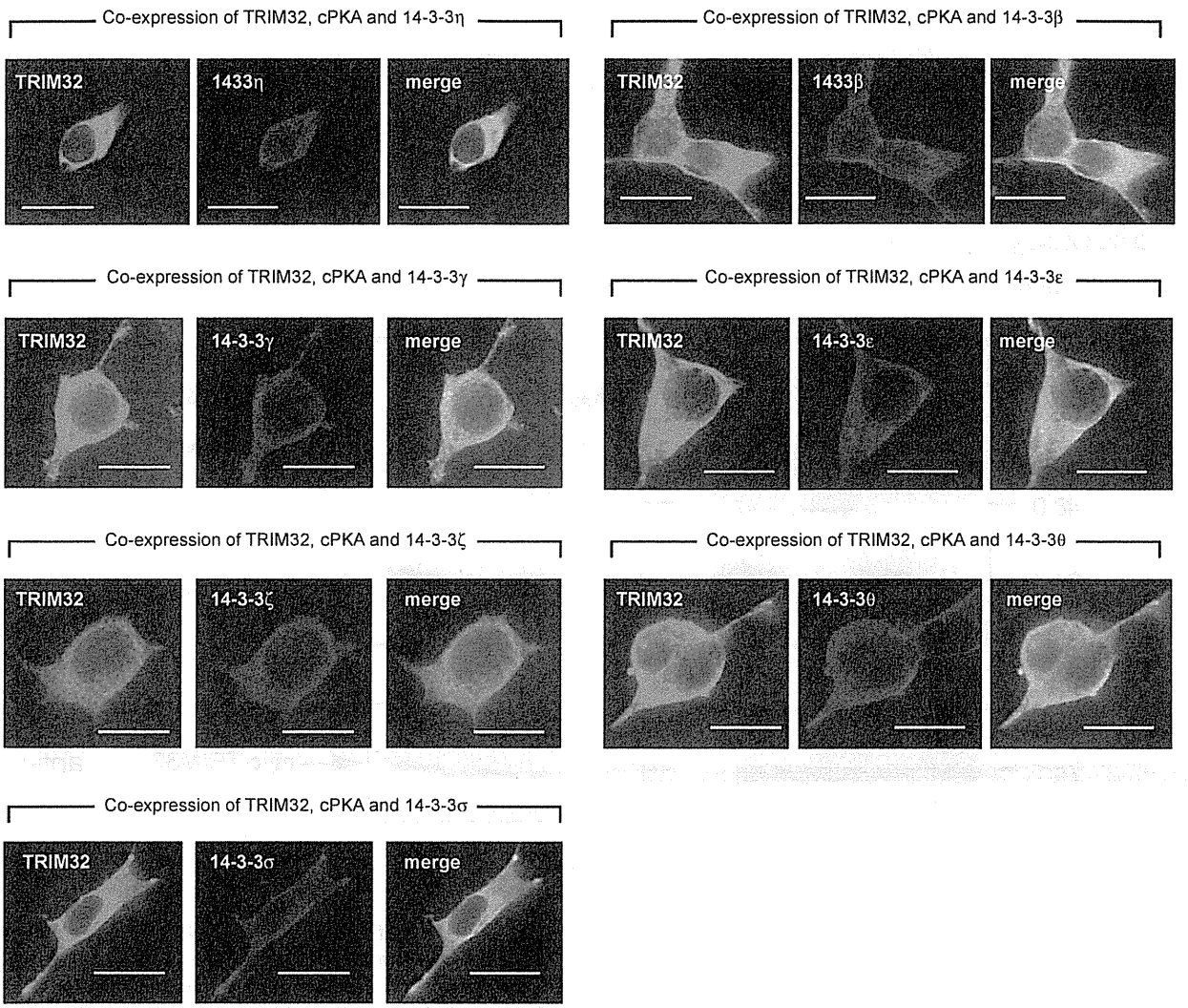


**Fig. S4. All mammalian 14-3-3 isoforms affect the subcellular distribution of TRIM32.** HEK293 cells were co-transfected with the indicated constructs (FLAG-TRIM32, myc-14-3-3s, cPKA), and after 24 h the cells were stained as in Fig. 3B. Scale bars: 10 μm.

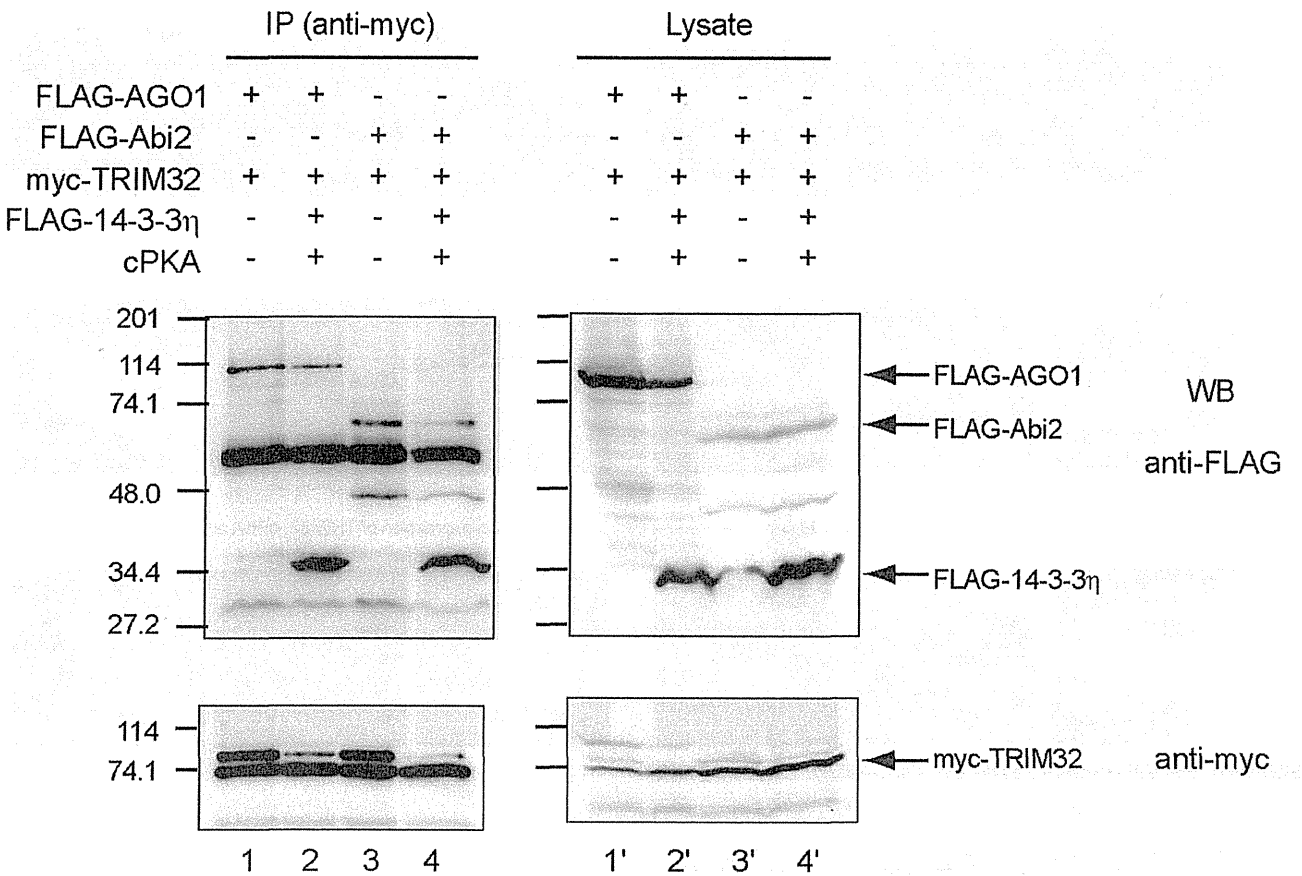


**Fig. S5. 14-3-3 binding does not significantly disrupt the interaction of TRIM32 with AGO1 or Abi2.** HEK293 cells transiently transfected with the indicated plasmids (5 μg each) were lysed with 1% Triton X-100 and then subjected to immunoprecipitation (IP) with anti-myc after normalizing levels of expressed proteins in each IP experiment. The amounts of myc- and FLAG-tagged proteins in the immunoprecipitates (left panels) and in lysates (right panels) were analyzed by western blotting (WB) with the indicated antibodies. Molecular size markers, in kDa, are indicated to the left.

**Table S1. List of 14-3-3-associated proteins consistently identified in at least two LC-MS/MS analyses**

Download Table S1

HEPATOLOGY
Official Journal of the American Association for the Study of Liver Diseases

# Polymorphisms of the Core, NS3, and NS5a Proteins of Hepatitis C Virus Genotype 1b Associate With Development of Hepatocellular Carcinoma

Ahmed El-Shamy,[1,2]* Michiko Shindo,[3]** Ikuo Shoji,[1] Lin Deng,[1] Tadao Okuno,[3] and Hak Hotta[1]

**Hepatocellular carcinoma (HCC) is one of the common sequelae of hepatitis C virus (HCV) infection. It remains controversial, however, whether HCV itself plays a direct role in the development of HCC. Although HCV core, NS3, and NS5A proteins were reported to display tumorigenic activities in cell culture and experimental animal systems, their clinical impact on HCC development in humans is still unclear. In this study we investigated sequence polymorphisms in the core protein, NS3, and NS5A of HCV genotype 1b (HCV-1b) in 49 patients who later developed HCC during a follow-up of an average of 6.5 years and in 100 patients who did not develop HCC after a 15-year follow-up. Sequence analysis revealed that Gln at position 70 of the core protein (core-Gln$^{70}$), Tyr at position 1082 plus Gln at 1112 of NS3 (NS3-Tyr$^{1082}$/Gln$^{1112}$), and six or more mutations in the interferon/ribavirin resistance-determining region of NS5A (NS5A-IRRDR≥6) were significantly associated with development of HCC. Multivariate analysis identified core-Gln$^{70}$, NS3-Tyr$^{1082}$/Gln$^{1112}$, and α-fetoprotein (AFP) levels (>20 ng/L) as independent factors associated with HCC. Kaplan-Meier analysis revealed a higher cumulative incidence of HCC for patients infected with HCV isolates with core-Gln$^{70}$, NS3-Tyr$^{1082}$/Gln$^{1112}$ or both than for those with non-(Gln$^{70}$ plus NS3-Tyr$^{1082}$/Gln$^{1112}$). In most cases, neither the residues at position 70 of the core protein nor positions 1082 and 1112 of the NS3 protein changed during the observation period. *Conclusion*: HCV isolates with core-Gln$^{70}$ and/or NS3-Tyr$^{1082}$/Gln$^{1112}$ are more closely associated with HCC development compared to those with non-(Gln$^{70}$ plus NS3-Tyr$^{1082}$/Gln$^{1112}$). (HEPATOLOGY 2013;58:555-563)**

See Editorial on Page 491

Hepatitis C virus (HCV) is a major etiologic agent of chronic hepatitis worldwide, with the estimated number of infected individuals being more than 180 million. Approximately 15% to 20% of chronically infected individuals undergo liver cirrhosis in a decade or so after infection, with hepatocellular carcinoma (HCC) arising from cirrhosis at an estimated rate of 1% to 4% per year.[1-3] Several host factors such as male gender, older age, elevated α-fetoprotein (AFP) level, advanced liver fibrosis as well as nonresponsiveness to interferon (IFN) therapy have been reported as important predictors of HCC development.[4,5] Recently, a host genetic factor, i.e., the *DEPDC5* locus polymorphism, was reported to be associated with progression to HCC in HCV-infected individuals.[6] On the other hand, it remains controversial as to whether HCV itself plays a direct role in the development of HCC. Experimental data suggest that HCV contributes to HCC by modulating pathways that promote malignant transformation of hepatocytes. HCV core, NS3, and NS5A proteins were shown to be involved in a

*Abbreviations: HCC, hepatocellular carcinoma; HCV, hepatitis C virus; IFN, interferon; IRRDR, interferon/ribavirin resistance-determining region; ISDR, interferon sensitivity-determining region.*

*From the [1]Division of Microbiology, Kobe University Graduate School of Medicine, Kobe, Japan; [2]Department of Virology, Suez Canal University Faculty of Veterinary Medicine, Ismalia, Egypt; and [3]Department of Gastroenterology, Akashi City Hospital, Akashi, Japan.*

*Received September 3, 2012; accepted December 9, 2012.*

*Supported in part by Health and Labour Sciences Research Grants from the Ministry of Health, Labour and Welfare, Japan, and a SATREPS Grant from Japan Science and Technology Agency (JST) and Japan International Cooperation Agency (JICA). This study was also carried out as part of Japan Initiative for Global Research Network on Infectious Diseases (J-GRID), Ministry of Education, Culture, Sports, Science and Technology, Japan, and the Global Center of Excellence (G-COE) Program at Kobe University Graduate School of Medicine.*

*These authors contributed equally to this work.

*Current address for Ahmed El-Shamy: Division of Liver Diseases, Mount Sinai School of Medicine, New York, New York, USA.*

*Current address for Michiko Shindo and Tadao Okuno: Okuno Gastroenterology Clinic, Akashi, Hyogo, Japan.*

number of potentially oncogenic pathways in cell culture and experimental animal systems.[7] HCV core protein rendered cultured cells more resistant to apoptosis[8,9] and promoted *ras* oncogene-mediated transformation.[10,11] Moreover, transgenic mice expressing the HCV core protein in the liver developed HCC.[12] However, the clinical impact of HCV proteins on HCC development in humans and whether all HCV isolates are equally associated with HCC is yet to be determined. In a clinical setting, HCV core protein mutations at positions 70 ($Gln^{70}$) and/or 91 ($Met^{91}$) were closely associated with HCC development.[13-16] $Gln^{70}$ and/or $Met^{91}$ were also linked to resistance to PEG-IFN/ribavirin (RBV) treatment.[17-20] In addition, we and other investigators reported that an N-terminal part of the NS3 protein has the capacity to transform NIH3T3 and rat fibroblast cells[21,22] and to render NIH3T3 cells more resistant to DNA damage-induced apoptosis, which is thought to be a prerequisite for malignant transformation of the cell.[23] Also, the NS5A protein is a pleiotropic protein with key roles in both viral RNA replication and modulation of the host cell functions.[24] In particular, the links between NS5A and the IFN responses have been widely discussed. It was proposed initially that sequence variations within a region in NS5A spanning from amino acids (aa) 2209 to 2248, called the IFN sensitivity-determining region (ISDR), were correlated with IFN responsiveness.[25] Subsequently, in the era of PEG-IFN/RBV combination therapy, we identified a new region near the C-terminus of NS5A spanning from aa 2334 to 2379, which we referred to as the IFN/RBV resistance-determining region (IRRDR).[26,27] The degree of sequence variations within the IRRDR was significantly associated with the clinical outcome of PEG-IFN/RBV therapy. In the context of HCC, several retrospective studies suggested that IFN-based therapy might reduce the risk of HCC development.[4,28-30]

In an attempt to clarify whether viral factors, in particular those within the core, NS3, and NS5A proteins, are involved in HCC development, we carried out a comparative analysis of the aa sequences obtained from HCV patients who developed HCC and those who did not. In addition, we studied the sequence evolution of these genes in the interval between chronic hepatitis C and HCC development over a period of 15 years.

## Patients and Methods

***Ethics Statement.*** The study protocol, which conforms to the provisions of the 1975 Declaration of Helsinki, was approved beforehand by the Ethic Committees in Akashi City Hospital and Kobe University Graduate School of Medicine, and written informed consent was obtained from each patient enrolled in this study.

***Patients.*** A total of 49 HCV-infected patients who developed HCC (HCC group) were retrospectively examined. They were followed up (from 1988 to 2003) with an average period until HCC development being 6.5 ± 2,9 years. Paired serum samples at the time of chronic hepatitis C (pre-HCC sample) and HCC development (post-HCC sample) were collected. As a control group, 100 HCV-infected patients who were followed up over a period of 15 years (from 1988 to 2003) without HCC development were retrospectively examined. Serum samples of the control group were available at the time of first visit to the clinic. All patients enrolled in this study were chronically infected with HCV genotype 1b (HCV-1b). HCV subtype was determined as reported previously.[31] Serum HCV RNA titers were quantitated by reverse-transcription polymerase chain reaction (RT-PCR0 with an internal RNA standard derived from the 5′ noncoding region of HCV (Amplicor HCV Monitor test, v. 2.0, Roche Diagnostics, Tokyo, Japan). All patients underwent liver biopsy and were diagnosed as chronic hepatitis. All HCC and 68% (68/100) of non-HCC patients received IFN-monotherapy, either natural IFN alpha (Sumiferon, Dainipponsumitomo Pharmaceutical, Osaka, Japan) at a dose of 6 million units (MU) or recombinant IFN alpha 2b (Intron A; Schering-Plough, Osaka, Japan) at a dose of 10 MU, 3 times a week for 6 months. All HCC patients were nonresponders (NR), who had detectable viremia during the entire course of IFN treatment. On the other hand, 18 (26%) of the 68 non-HCC patients treated with IFN achieved HCV RNA negativity at the end of treatment followed by rebound viremia within 6 months after the treatment and, therefore, they were referred to as relapsers. The other 50 IFN-treated, non-HCC patients were NR. The remaining 32 non-HCC patients did not receive IFN. All patients were

*Address reprint requests to: Hak Hotta, M.D., Ph.D., Division of Microbiology, Kobe University Graduate School of Medicine, 7-5-1 Kusunoki-cho, Chuo-ku, Kobe 650-0017, Japan. E-mail: hotta@kobe-u.ac.jp; fax: +81-78-382-5519.*

*View this article online at wileyonlinelibrary.com.*
*DOI 10.1002/hep.26205*
*Potential conflict of interest: Nothing to report.*

seen every 2 months and tested for liver function markers during the follow-up period.

***Sequence Analysis of HCV Core, NS3, and NS5A Proteins.*** HCV RNA was extracted from 140 $\mu$L of serum using a commercially available kit (QIAmp viral RNA kit; Qiagen, Tokyo, Japan). The core, NS3, and NS5A regions of the HCV genome were amplified as described elsewhere.[26,32-34] The sequences of the amplified fragments were determined by direct sequencing. The aa sequences were deduced and aligned using GENETYX Win software version 7.0 (GENETYX, Tokyo, Japan). The numbering of aa was according to the polyprotein of the prototype of HCV-1b; HCV-J.[35]

***Statistical Analysis.*** Statistical differences in the baseline parameters of HCC and control groups were determined by Student's $t$ test for numerical variables and Fisher's exact probability or chi-square tests for categorical variables. Likewise, statistical differences in viral mutations between HCC and control groups were determined by Fisher's exact probability test. Kaplan-Meier analysis was performed to estimate the cumulative incidence of HCC. The data obtained were evaluated by the log-rank test. Univariate and multivariate logistic analyses were performed to identify variables that independently associated with HCC development. Variables with $P < 0.1$ in univariate analysis were included in a backward stepwise multivariate logistic regression analysis. The odds ratios and 95% confidence intervals (95% CI) were calculated. All statistical analyses were performed using SPSS v. 16 software (Chicago, IL). Unless otherwise stated, $P < 0.05$ was considered statistically significant.

***Nucleotide Sequence Accession Numbers.*** The sequence data reported in this article have been deposited in the DDBJ/EMBL/GenBank nucleotide sequence databases with the accession numbers AB719460 through AB719842.

## Results

***Demographic Characteristics of HCC and Control Groups.*** The clinical characteristics of HCC and control groups are shown in Table 1. The HCC group had significantly higher titers of ALT, AST, and AFP, and higher fibrosis staging score than that of the control group. There was no significant difference in viremia titers between the two groups.

***Correlation Between Core Protein Sequence Polymorphism and HCC Development.*** HCV core protein sequences were obtained from all (49/49) and 94% (94/100) of pre-HCC and control patients' sera, respectively. Comparative sequence analysis revealed that 22 (45%) of 49 HCV isolates in the pre-HCC sera (pre-HCC isolates) and 59 (63%) of 94 HCV isolates from the control group (control isolates) had wild-core ($Arg^{70}/Leu^{91}$) (Table 2). The difference between HCC and control groups was hovering at a statistically significant level ($P = 0.05$). When the sequence pattern at position 70 alone was examined, a stronger association with HCC was observed. We found that 21 (43%) of 49 pre-HCC isolates had $Gln^{70}$ while only 13 (14%) of 94 control isolates did ($P = 0.0002$). On the other hand, there was no significant correlation between sequence pattern at position 91 and HCC. Thus, a single mutation at position 70 ($Gln^{70}$) was the only polymorphic factor within core protein that was significantly associated with HCC development. It should be noted that there was no significant correlation between $Gln^{70}$ and the degree of fibrosis progression (data not shown).

**Table 1. Demographic Characteristics of HCC and Control Groups**

| Factor | HCC | Control | *P* Value |
|---|---|---|---|
| Age | 57.3 ± 7.0* | 56.4 ± 8.3 | 0.54 |
| Sex (male/female) | 31/18 | 54/46 | 0.29 |
| ALT (IU/L) | 159.4 ± 79.8 | 129.7 ± 51.5 | 0.007 |
| AST (IU/L) | 113.0 ± 62.2 | 91.6 ± 44.1 | 0.017 |
| AFP (ng/L) | 29.1 ± 33.7 | 18.4 ± 4.4 | 0.002 |
| Platelets (x $10^4/mm^3$) | 16.2 ± 2.8 | 16.2 ± 2.4 | 0.88 |
| Inflammation grading score | 8.7 ± 0.9 | 8.4 ± 1.2 | 0.05 |
| Fibrosis staging score | 2.4 ± 0.5 | 2.2 ± 0.5 | 0.02 |
| HCV-RNA (KIU/mL) | 593.4 ± 112.3 | 618.1 ± 95.9 | 0.17 |

*Mean ± SD. HCC, hepatocellular carcinoma; ALT, alanine aminotransferase; AST, aspartate transaminase; AFP; $\alpha$-fetoprotein.

***Correlation Between NS3 Protein Sequence Polymorphism and HCC Development.*** Sequences of NS3 serine protease domain (aa 1027 to 1146) were obtained from 94% (46/49) and 93% (93/100) of pre-HCC and control isolates, respectively. We found that 29 (63%) of 46 pre-HCC isolates had Tyr and Gln at positions 1082 and 1112, respectively ($Tyr^{1082}/Gln^{1112}$), while 39 (42%) of 93 control isolates did (Table 2). The difference in the proportion between pre-HCC and control isolates was statistically significant ($P = 0.029$). On the other hand, there was no significant correlation between $Tyr^{1082}/Gln^{1112}$ and the degree of fibrosis progression (data not shown).

***Correlation Between NS5A Protein Sequence Polymorphism and HCC Development.*** NS5A protein sequences were obtained from 92% (45/49) and 74% (74/100) of pre-HCC and control isolates, respectively. Twenty-four (53%) of 45 pre-HCC isolates had IRRDR of 6 or more mutations (IRRDR≥6)

**Table 2. Correlation Between HCC and Sequence Polymorphic Factors of Core, NS3 and NS5A**

| HCV Protein | Factor | No. of Subjects / No. of Total* HCC | Control | P Value |
|---|---|---|---|---|
| Core | Wild-core ($Arg^{70}$/$Leu^{91}$) | 22/49 (45%) | 59/94 (63%) | 0.05 |
| | Non-wild-core | 27/49 (55%) | 35/94 (37%) | |
| | $Gln^{70}$ | 21/49 (43%) | 13/94 (14%) | 0.0002 |
| | Non-$Gln^{70}$ | 28/49 (57%) | 81/94 (86%) | |
| | $Leu^{91}$ | 37/49 (76%) | 70/94 (74%) | 1.0 |
| | Non- $Leu^{91}$ | 12/49 (24%) | 24/94 (26%) | |
| NS3 | $Tyr^{1082}$ / $Gln^{1112}$ | 29/46 (63%) | 39/93 (42%) | 0.029 |
| | Non-($Tyr^{1082}$ / $Gln^{1112}$) | 17/46 (37%) | 54/93 (58%) | |
| NS5A | IRRDR≥6 | 24/45 (53%) | 15/74 (20%) | 0.0003 |
| | IRRDR≤5 | 21/45 (47%) | 59/74 (80%) | |
| | ISDR≥3 | 11/45 (24%) | 8/74 (11%) | 0.07 |
| | ISDR≤2 | 34/45 (76%) | 66/74 (89%) | |
| | $Asn^{2218}$ | 11/45 (24%) | 3/74 (4%) | 0.002 |
| | Non-$Asn^{2218}$ | 34/45 (76%) | 71/74 (96%) | |

*Number of subjects with a given factor / total number of HCC or control. HCC, hepatocellular carcinoma; $Arg^{70}$, arginine at position 70 of the core protein; $Leu^{91}$, leucine at position 91 of the core protein; $Gln^{70}$, glutamine at position 70 of the core protein; $Tyr^{1082}$, tyrosine at position 1082 of NS3; $Gln^{1112}$, glutamine at position 1112 of NS3; IRRDR, interferon/ribavirin resistance-determining region; ISDR, interferon sensitivity-determining region; $Asn^{2218}$, asparagine at position 2218 of NS5A-ISDR.

while only 15 (20%) of 74 control isolates did (Table 2; $P = 0.0003$). We also found that pre-HCC isolates tended to have a higher degree of sequence heterogeneity in ISDR than control isolates, although not statistically significant due probably to the small number of cases examined; 11 (24%) of 45 pre-HCC isolates and 8 (11%) of 74 of control isolates had ISDR with three or more mutations ($P = 0.07$). Moreover, Asn at position 2218 ($Asn^{2218}$) within the ISDR was found in 24% (11/45) of pre-HCC isolates and only in 4% (3/74) of the control isolates ($P = 0.002$), suggesting that $Asn^{2218}$ is significantly associated with development of HCC.

***Cumulative HCC Incidence on the Basis of Core-$Gln^{70}$, NS3-$Tyr^{1082}$/$Gln^{1112}$, NS5A-IRRDR≥6, and NS5A-$Asn^{2218}$.*** Follow-up study revealed that the cumulative HCC incidence in patients infected with HCV-1b isolates with core protein of $Gln^{70}$ and those of non-$Gln^{70}$, respectively, was 29% and 5% at the end of 5 years, 56% and 23% at the end of 10 years, and 63% and 26% at the end of 15 years (Fig. 1A), with the differences between the two groups being statistically significant ($P < 0.0001$; Log-rank test). Likewise, the cumulative HCC incidence in patients infected with HCV-1b isolates with NS3 of $Tyr^{1082}$/$Gln^{1112}$ and those of non-($Tyr^{1082}$/$Gln^{1112}$), respectively, was 15% and 7% at the end of 5 years, 37% and 24% at the end of 10 years, and 45% and 24% at the end of 15 years ($P = 0.02$) (Fig. 1B). Also, the cumulative HCC incidence in patients infected with HCV-1b isolates of IRRDR≥6 and those of IRRDR≤5, respectively, was 18% and 10% at the end of 5 years, 59% and 22% at the end of 10 years, and 63% and 27% at the end of 15 years ($P = 0.0002$) (Fig. 1C). Similarly, the cumulative HCC incidence in patients infected with HCV-1b isolates of $Asn^{2218}$ and those of non-$Asn^{2218}$, respectively, was 31% and 9% at the end of 5 years, 77% and 28% at the end of 10 years, and 77% and 33% at the end of 15 years ($P = 0.0003$) (Fig. 1D).

***Identification of Independent Factors Correlated With HCC Development by Univariate and Multivariate Logistic Regression Analyses.*** In order to identify significant independent factors associated with HCC development, all available data of baseline patients' parameters and core, NS3, and NS5A polymorphic factors were first analyzed by univariate logistic analysis. This analysis yielded eight factors that were significantly associated with HCC development: core-$Gln^{70}$, NS3-($Tyr^{1082}$/$Gln^{1112}$), NS5A-IRRDR≥6, NS5A-$Asn^{2218}$, increased levels of ALT (>165 IU/L), AST (>65 IU/L), and AFP (>20 ng/L), and fibrosis staging score (≥3). Subsequently, those eight factors were entered in multivariate logistic regression analysis. This analysis identified two viral factors, core-$Gln^{70}$ and NS3-($Tyr^{1082}$/$Gln^{1112}$), and a host factor, AFP levels (>20 ng/L), as independent factors associated with HCC development (Table 3).

The vast majority of pre-HCC isolates (85%; 39/46) had core-$Gln^{70}$ and/or NS3-$Tyr^{1082}$/$Gln^{1112}$ and only 15% (7/46) had non-($Gln^{70}$ plus NS3-$Tyr^{1082}$/$Gln^{1112}$). By contrast, about a half of control isolates (52%; 46/89) had non-($Gln^{70}$ plus NS3-$Tyr^{1082}$/$Gln^{1112}$) (Fig. 2A). The difference in the proportion between HCC and control groups was statistically significant ($P < 0.0001$). Furthermore, the cumulative HCC incidence after 15-year follow-up was highest (63%) among patients with core-$Gln^{70}$ plus NS3-($Tyr^{1082}$/$Gln^{1112}$), whereas it was lowest (11%) among patients with non-($Gln^{70}$ plus NS3-$Tyr^{1082}$/$Gln^{1112}$) (Fig. 2B), with the difference being statistically significant ($P < 0.0001$; Log-rank test).

***Evolution of the Sequences of the Core, NS3, and NS5A Proteins During the Follow-up Period From Chronic Hepatitis to HCC Development.*** Finally, we investigated sequence evolution of the core protein, NS3 and NS5A (IRRDR and ISDR) during the follow-up period from chronic hepatitis to HCC development by comparing the sequences between pre-HCC and

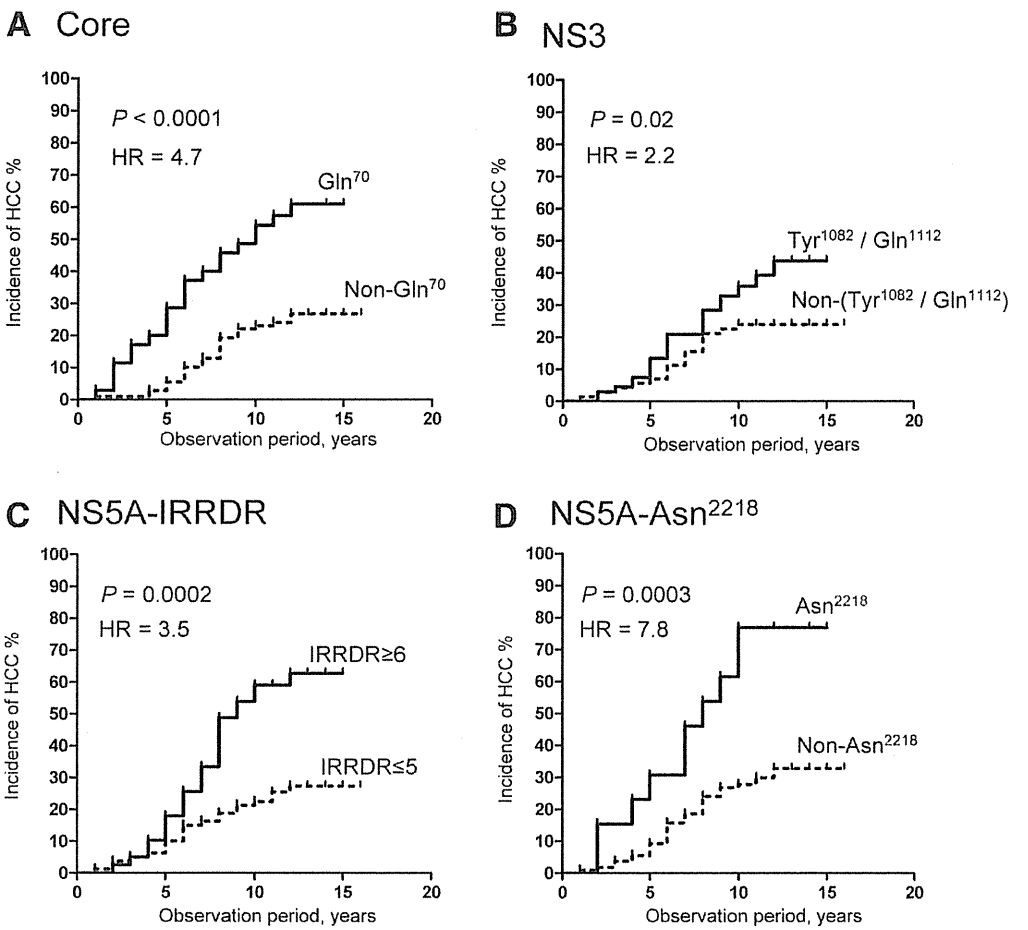


Fig. 1. Cumulative HCC incidence on the basis of HCV-1b sequence patterns. (A) Position 70 of the core protein. The numbers of core-$Gln^{70}$ and non-$Gln^{70}$ analyzed were 34 and 109, respectively. (B) Positions 1082 and 1112 of NS3. The numbers of NS3-($Tyr^{1082}$/$Gln^{1112}$) and non-($Tyr^{1082}$/$Gln^{1112}$) analyzed were 68 and 71, respectively. (C) NS5A-IRRDR. The numbers of NS5A-IRRDR≥6 and IRRDR≤5 analyzed were 39 and 80, respectively. (D) NS5A-$Asn^{2218}$. The numbers of NS5A-$Asn^{2218}$ and non-$Asn^{2218}$ analyzed were 14 and 105, respectively.

post-HCC isolates. The residue at position 70 of the core protein was conserved in 91% (41/45) of sequence pairs analyzed. The substitutions observed at this position were from $Arg^{70}$ and $His^{70}$ each to $Gln^{70}$ in two cases and from $Gln^{70}$ to $Arg^{70}$ in the other two cases. The residues at positions 1082 and 1112 of NS3 were conserved in 95% (41/43) and 100% (43/43), respectively, of the sequence pairs analyzed.

**Table 3. Univariate and Multivariate Regression Analyses to Identify Independent Factors Associated With HCC**

| | Univariate | | Multivariate | |
|---|---|---|---|---|
| Variable | Odds Ratio (95% CI) | P Value | Odds Ratio (95% CI) | P Value |
| Core-$Gln^{70}$ | 0.23 (0.10 - 0.52) | 0.0004 | 6.8 (2.1 - 23.0) | 0.001 |
| NS3-$Tyr^{1082}$ / $Gln^{1112}$ | 2.4 (1.1 - 4.9) | 0.029 | 3.4 (1.1 - 10.0) | 0.03 |
| NS5A-IRRDR≥6 | 4.5 (2.0 - 10.0) | 0.0003 | | |
| NS5A-$Asn^{2218}$ | 7.7 (2.0 - 29.0) | 0.002 | | |
| AFP (>20 ng/L) | 12 (5.1 - 30.0) | 0.0001 | 19.5 (4.7 - 80.0) | 0.0001 |
| ALT (>165 IU/L) | 4.0 (1.8 - 8.6) | 0.0006 | | |
| AST (>65 IU/L) | 3.9 (1.5 - 10.0) | 0.003 | | |
| Fibrosis staging score (≥3) | 2.4 (1.1 - 4.9) | 0.02 | | |

$Gln^{70}$, glutamine at position 70 of the core protein; $Tyr^{1082}$, tyrosine at position 1082 of NS3; $Gln^{1112}$, glutamine at position 1112 of NS3; IRRDR, interferon/ribavirin resistance-determining region; $Asn^{2218}$, asparagine at position 2218 of NS5A-ISDR, ALT, alanine aminotransferase; AST, aspartate transaminase; AFP; α-fetoprotein; IFN; interferon.

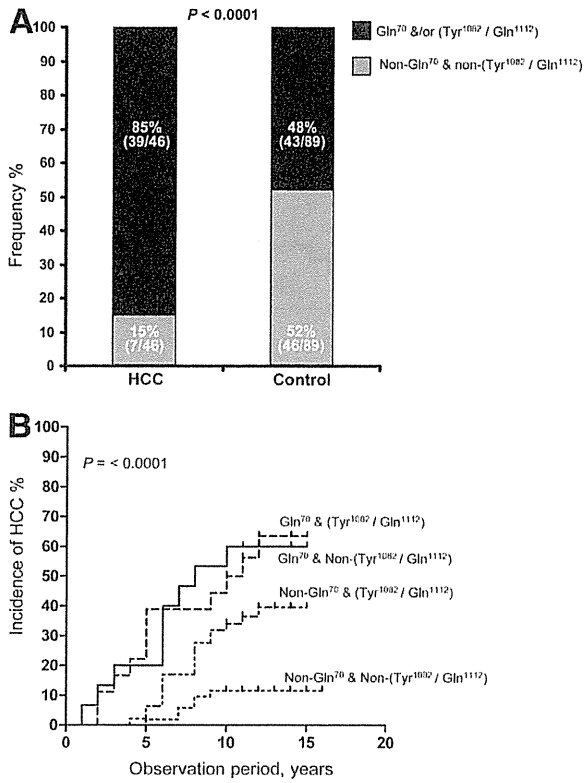


Fig. 2. (A) Proportions of HCV-1b isolates of the HCC high-risk group (core-Gln$^{70}$ and/or NS3-[Tyr$^{1082}$/Gln$^{1112}$]) and the low-risk group (non-Gln$^{70}$ and non-[Tyr$^{1082}$/Gln$^{1112}$]) among HCC and control groups. (B) Cumulative HCC incidence on the basis of different combined sequence patterns of position 70 of the core protein and positions 1082 and 1112 of NS3. Core-Gln$^{70}$ and NS3-(Tyr$^{1082}$/Gln$^{1112}$), n = 18; core-Gln$^{70}$ and non-(Tyr$^{1082}$/Gln$^{1112}$), n = 16; non-Gln$^{70}$ and NS3-(Tyr$^{1082}$/Gln$^{1112}$), n = 48; non-Gln$^{70}$/non-(Tyr$^{1082}$/Gln$^{1112}$), n = 53.

IRRDR and ISDR showed a high degree of sequence evolution. IRRDR sequences were different between pre-HCC and post-HCC isolates in 66% (25/38) of cases analyzed (Fig. 3). IRRDR sequences tended to be more polymorphic at the time of HCC occurrence. Frequency of HCV isolates with IRRDR≥6 was significantly higher in post-HCC isolates than in pre-HCC isolates; IRRDR≥6 was found in 47% (18/38) of post-HCC isolates compared to 24% (9/38) of pre-HCC isolates ($P = 0.03$). On the other hand, ISDR≥3 was found in 21% (8/38) of post-HCC isolates compared to 11% (4/38) of pre-HCC isolates, with the difference between the two groups being not statistically significant ($P = 0.3$).

## Discussion

HCC is one of the common long-term complications of HCV infection. However, whether HCV itself plays a direct role in the development of HCC and whether all HCV isolates are equally associated with HCC development remain to be determined. HCV core, NS3, and NS5A proteins have been reported to affect a wide variety of potentially oncogenic pathways in cell culture and experimental animal systems.[7] In the present study, we demonstrated that HCV isolates with core-Gln$^{70}$, NS3-Tyr$^{1082}$/Gln$^{1112}$ or NS5A-IRRDR≥6 were closely associated with HCC development. In addition, a follow-up study revealed that sequence patterns at position 70 of the core protein and positions 1082 and 1112 of NS3 did not significantly alter during the progression from chronic hepatitis to HCC while NS5A-IRRDR showed a significantly higher degree of sequence heterogeneity in post-HCC than in pre-HCC isolates.

Correlation between polymorphisms at positions 70 and 91 of HCV-1b core protein and IFN-based treatment outcome was extensively studied, especially in a Japanese population.[17-20] Interestingly, the same mutations were also associated with progression to HCC in the Japanese population with HCV-1b infection.[13] Results obtained in the present study confirmed and emphasized the significant association between the mutation at position 70 (core-Gln$^{70}$), but not at position 91, and HCC development (Tables 2, 3; Fig. 1A). Despite the clinical evidence that strongly supports the correlation between core-Gln$^{70}$ and HCC development, the molecular mechanism underlying this correlation is still obscure. Delhem et al.[36] found that tumor-derived HCV core proteins, but not nontumor-derived ones, interact with and activate double-stranded RNA-dependent protein kinase (protein kinase R or PKR), which might modulate viral persistence and carcinogenesis. Gln$^{70}$ was found in two of the three tumor-derived sequences, whereas Arg$^{70}$ was found in two of the three nontumor-derived ones.

As for the NS3 protein of HCV, the possible link between an N-terminal portion of NS3 encoding viral serine protease (aa 1027 to 1146) and hepatocarcinogenesis was reported.[21,22] However, information about the relationship between NS3 sequence diversity and HCC development is still limited. We previously reported a significant correlation between predicted secondary structure of an N-terminal portion of NS3 and HCC development.[34] In the present study, we demonstrated that HCV patients infected with HCV isolates with NS3-(Tyr$^{1082}$/Gln$^{1112}$) were at a higher risk to develop HCC than those infected with HCV isolates with non-Tyr$^{1082}$/Gln$^{1112}$ (Tables 2, 3; Fig. 2B). Computer-assisted secondary structure analysis of NS3 revealed that Tyr$^{1082}$ was associated with the

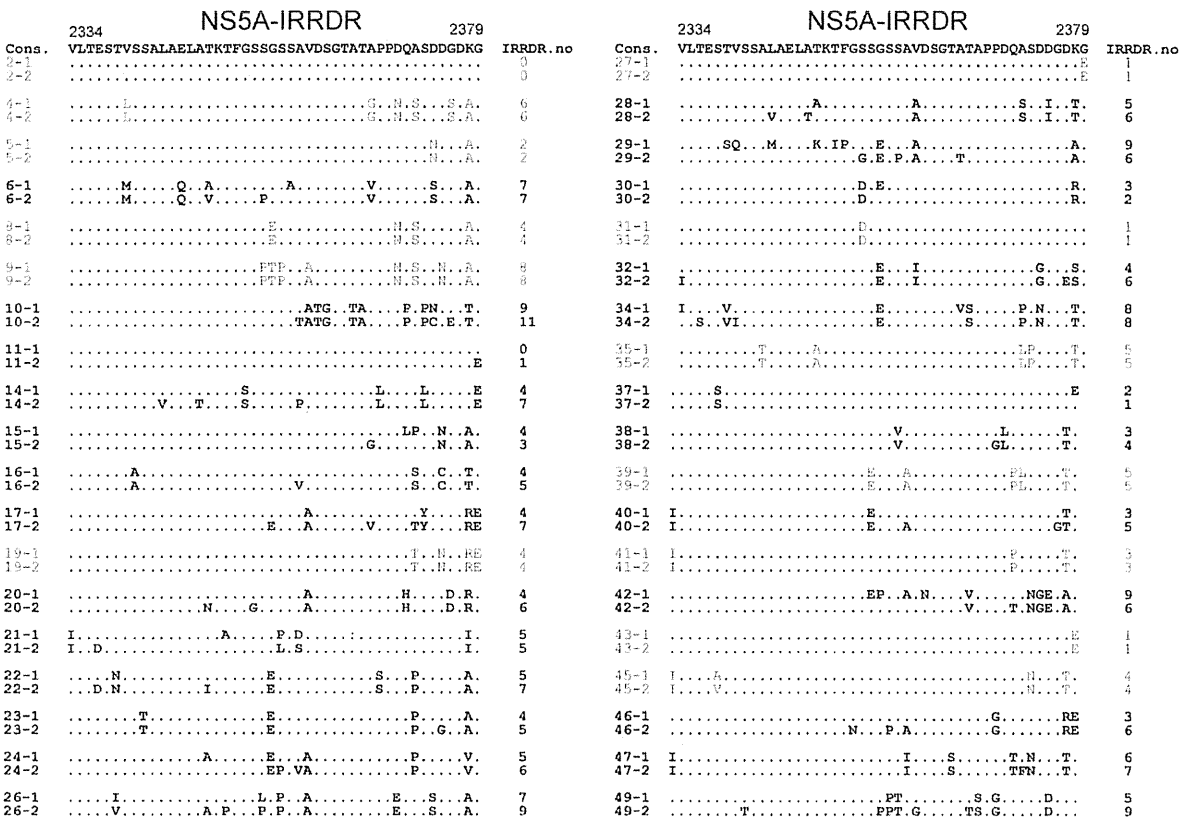


Fig. 3. Pairwise comparison of IRRDR sequences of HCV-1b during the follow-up period between chronic hepatitis and HCC development. Sequence pairs that differ between pre-HCC (numbered with -1) and post-HCC isolates (numbered with -2) are shown. The consensus sequence (Cons.) is shown at the top. The numbers along the sequence indicate the aa positions. Dots indicate residues identical to those of the Cons. sequence. The numbers of IRRDR mutations are shown on the right.

presence of a turn structure at around position 1083 while Phe[1082] was associated with the absence of the turn structure.[34] Notably, the catalytic triad of NS3 serine protease consists of His[1083], Asp[1107], and Ser[1165].[37] Since positions 1082 and 1112 are in close vicinity of the catalytic triad, sequences diversity at these positions might influence the serine protease activity and also pathogenicity of HCV. Large-scale, multicenter clinical studies as well as more detailed experimental studies at the molecular and cellular levels are needed to clarify the importance of sequence diversity at positions 1082 and 1112 of NS3 in HCV-mediated hepatocarcinogenesis.

HCV heterogeneity in NS5A-ISDR and NS5A-IRRDR are correlated with IFN-responsiveness.[17,18,25,26] As IFN-based therapy reduces the risk of HCC development,[4,28-30] we were interested to investigate whether there is a correlation between sequence heterogeneity in NS5A and development of HCC. Our present results revealed that a high degree of sequence heterogeneity in IRRDR (IRRDR≥6) was closely associated with HCC development (Table 2). We previously reported that IRRDR≥6 was significantly associated with good responses to PEG-IFN/RBV combination therapy.[26,27] These results collectively suggest that oncogenic properties and PEG-IFN/RBV responsiveness are independent viral characteristics and that PEG-IFN/RBV therapy helps eliminate oncogenic HCV isolates, thus reducing the risk of HCC development.

Position 2218 of NS5A, located within ISDR, appears to tolerate a wide range of aa substitutions as observed in different HCV-1b isolates.[25,38,39] Interestingly, Asn at position 2218 (Asn[2218]) was detected significantly more frequently in pre-HCC isolates than in the control isolates. Further studies are needed to determine the possible importance of this residue in hepatocarcinogenesis.

Another focus of attention is how the sequences of the core protein, NS3, and NS5A-IRRDR evolve during the interval between chronic hepatitis and HCC development. One of the significant advantages of the

present study was that we could conduct a longitudinal investigation by analyzing the target sequences of pre- and post-HCC isolates. We found that core-$Gln^{70}$ and NS3-($Tyr^{1082}$/$Gln^{1112}$) were well conserved in each paired sample. This indicates that core-$Gln^{70}$ and NS3-($Tyr^{1082}$/$Gln^{1112}$) were already present before the development of HCC. Non-$Gln^{70}$ of the core protein and non-$Tyr^{1082}$ and non-$Gln^{1112}$ of NS3 were also well conserved in each paired sample. These results imply the possibility that these sequence patterns were not a result of HCC but, rather, they were a possible causative factor for the development of HCC. We hypothesize, therefore, that HCV isolates with core-$Gln^{70}$ and/or NS3-($Tyr^{1082}$/$Gln^{1112}$) are highly oncogenic, whereas those with non-($Gln^{70}$ plus NS3-$Tyr^{1082}$/$Gln^{1112}$) are less oncogenic. It is not clear yet as to whether these oncogenic mutations were present from the very beginning of HCV infection or if they emerged at a certain timepoint (before the initiation of follow-up) during the long-term persistence through an adaptive viral evolution in the host. More comprehensive follow-up study is needed to address this issue. In any case, the core-$Gln^{70}$ and NS3-($Tyr^{1082}$/$Gln^{1112}$) would be considered an index for prediction of HCC development. On the other hand, IRRDR in NS5A is more tolerant for sequence evolution. IRRDR in post-HCC isolates showed a significantly higher degree of sequence heterogeneity compared with that in pre-HCC isolates. This observation suggests that IRRDR is under strong selective pressure during the course of HCV infection and that the high degree of IRRDR heterogeneity (IRRDR$\geq$6) in HCV isolates from patients with HCC may not be a causative factor for development of HCC.

In conclusion, the present results suggest the possibility that patients infected with HCV isolates with core-$Gln^{70}$ and/or NS3-($Tyr^{1082}$/$Gln^{1112}$) are at a higher risk to develop HCC compared to those with non-($Gln^{70}$ plus NS3-$Tyr^{1082}$/$Gln^{1112}$).

## References


1. Lauer GM, Walker BD. Hepatitis C virus infection. N Engl J Med 2001;345:41-52.
2. Niederau C, Lange S, Heintges T, Erhardt A, Buschkamp M, Hurter D, et al. Prognosis of chronic hepatitis C: results of a large, prospective cohort study. HEPATOLOGY 1998;28:1687-1695.
3. Ikeda K, Saitoh S, Suzuki Y, Kobayashi M, Tsubota A, Koida I, et al. Disease progression and hepatocellular carcinogenesis in patients with chronic viral hepatitis: a prospective observation of 2215 patients. J Hepatol 1998;28:930-938.
4. Yoshida H, Shiratori Y, Moriyama M, Arakawa Y, Ide T, Sata M, et al. Interferon therapy reduces the risk for hepatocellular carcinoma: national surveillance program of cirrhotic and noncirrhotic patients with chronic hepatitis C in Japan. IHIT Study Group. Inhibition of hepatocarcinogenesis by interferon therapy. Ann Intern Med 1999;131: 174-181.
5. Lok AS, Seeff LB, Morgan TR, di Bisceglie AM, Sterling RK, Curto TM, et al. Incidence of hepatocellular carcinoma and associated risk factors in hepatitis C-related advanced liver disease. Gastroenterology 2009;136:138-148.
6. Miki D, Ochi H, Hayes CN, Abe H, Yoshima T, Aikata H, et al. Variation in the DEPDC5 locus is associated with progression to hepatocellular carcinoma in chronic hepatitis C virus carriers. Nat Genet 2011; 43:797-800.
7. Banerjee A, Ray RB, Ray R. Oncogenic potential of hepatitis C virus proteins. Viruses 2010;2:2108-2133.
8. Marusawa H, Hijikata M, Chiba T, Shimotohno K. Hepatitis C virus core protein inhibits Fas- and tumor necrosis factor alpha-mediated apoptosis via NF-κB activation. J Virol 1999;73:4713-4720.
9. Ray RB, Meyer K, Ray R. Suppression of apoptotic cell death by hepatitis C virus core protein. Virology 1996;226:176-182.
10. Chang J, Yang SH, Cho YG, Hwang SB, Hahn YS, Sung YC. Hepatitis C virus core from two different genotypes has an oncogenic potential but is not sufficient for transforming primary rat embryo fibroblasts in cooperation with the H-*ras* oncogene. J Virol 1998;72: 3060-3065.
11. Ray RB, Lagging LM, Meyer K, Ray R. Hepatitis C virus core protein cooperates with ras and transforms primary rat embryo fibroblasts to tumorigenic phenotype. J Virol 1996;70:4438-4443.
12. Moriya K, Fujie H, Shintani Y, Yotsuyanagi H, Tsutsumi T, Ishibashi K, et al. The core protein of hepatitis C virus induces hepatocellular carcinoma in transgenic mice. Nat Med 1998;4:1065-1067.
13. Akuta N, Suzuki F, Kawamura Y, Yatsuji H, Sezaki H, Suzuki Y, et al. Amino acid substitutions in the hepatitis C virus core region are the important predictor of hepatocarcinogenesis. HEPATOLOGY 2007;46: 1357-1364.
14. Akuta N, Suzuki F, Hirakawa M, Kawamura Y, Sezaki H, Suzuki Y, et al. Amino acid substitutions in hepatitis C virus core region predict hepatocarcinogenesis following eradication of HCV RNA by antiviral therapy. J Med Virol 2011;83:1016-1022.
15. Akuta N, Suzuki F, Kawamura Y, Yatsuji H, Sezaki H, Suzuki Y, et al. Substitution of amino acid 70 in the hepatitis C virus core region of genotype 1b is an important predictor of elevated alpha-fetoprotein in patients without hepatocellular carcinoma. J Med Virol 2008;80: 1354-1362.
16. Kobayashi M, Akuta N, Suzuki F, Hosaka T, Sezaki H, Kobayashi M, et al. Influence of amino-acid polymorphism in the core protein on progression of liver disease in patients infected with hepatitis C virus genotype 1b. J Med Virol 2010;82:41-48.
17. El-Shamy A, Shoji I, Saito T, Watanabe H, Ide YH, Deng L, et al. Sequence heterogeneity of NS5A and core proteins of hepatitis C virus and virological responses to pegylated-interferon/ribavirin combination therapy. Microbiol Immunol 2011;55:418-426.
18. El-Shamy A, Kim SR, Ide YH, Sasase N, Imoto S, Deng L, et al. Polymorphisms of hepatitis C virus non-structural protein 5A and core protein and clinical outcome of pegylated-interferon/ribavirin combination therapy. Intervirology 2012;55:1-11.
19. Akuta N, Suzuki F, Sezaki H, Suzuki Y, Hosaka T, Someya T, et al. Association of amino acid substitution pattern in core protein of hepatitis C virus genotype 1b high viral load and non-virological response to interferon-ribavirin combination therapy. Intervirology 2005;48: 372-380.
20. Akuta N, Suzuki F, Kawamura Y, Yatsuji H, Sezaki H, Suzuki Y, et al. Predictive factors of early and sustained responses to peginterferon plus ribavirin combination therapy in Japanese patients infected with hepatitis C virus genotype 1b: amino acid substitutions in the core region and low-density lipoprotein cholesterol levels. J Hepatol 2007;46: 403-410.

21. Sakamuro D, Furukawa T, Takegami T. Hepatitis C virus nonstructural protein NS3 transforms NIH 3T3 cells. J Virol 1995;69:3893-3896.
22. Zemel R, Gerechet S, Greif H, Bachmatove L, Birk Y, Golan-Goldhirsh A, et al. Cell transformation induced by hepatitis C virus NS3 serine protease. J Viral Hepat 2001;8:96-102.
23. Fujita T, Ishido S, Muramatsu S, Itoh M, Hotta H. Suppression of actinomycin D-induced apoptosis by the NS3 protein of hepatitis C virus. Biochem Biophys Res Commun 1996;229:825-831.
24. Macdonald A, Harris M. Hepatitis C virus NS5A: tales of a promiscuous protein. J Gen Virol 2004;85:2485-2502.
25. Enomoto N, Sakuma I, Asahina Y, Kurosaki M, Murakami T, Yamamoto C, et al. Mutations in the nonstructural protein 5A gene and response to interferon in patients with chronic hepatitis C virus 1b infection. N Engl J Med 1996;334:77-81.
26. El-Shamy A, Nagano-Fujii M, Sasase N, Imoto S, Kim SR, Hotta H. Sequence variation in hepatitis C virus nonstructural protein 5A predicts clinical outcome of pegylated interferon/ribavirin combination therapy. HEPATOLOGY 2008;48:38-47.
27. Kim SR, El-Shamy A, Imoto S, Kim KI, Ide YH, Deng L, et al. Prediction of response to pegylated interferon/ribavirin combination therapy for chronic hepatitis C genotype 1b and high viral load. J Gastroenterol 2012;47:1143-1151.
28. Ikeda K, Saitoh S, Arase Y, Chayama K, Suzuki Y, Kobayashi M, et al. Effect of interferon therapy on hepatocellular carcinogenesis in patients with chronic hepatitis type C: A long-term observation study of 1,643 patients using statistical bias correction with proportional hazard analysis. HEPATOLOGY 1999;29:1124-1130.
29. Okanoue T, Itoh Y, Minami M, Sakamoto S, Yasui K, Sakamoto M, et al. Interferon therapy lowers the rate of progression to hepatocellular carcinoma in chronic hepatitis C but not significantly in an advanced stage: a retrospective study in 1148 patients. Viral Hepatitis Therapy Study Group. J Hepatol 1999;30:653-659.
30. Benvegnu L, Chemello L, Noventa F, Fattovich G, Pontisso P, Alberti A. Retrospective analysis of the effect of interferon therapy on the clinical outcome of patients with viral cirrhosis. Cancer 1998;83:901-909.
31. Okamoto H, Sugiyama Y, Okada S, Kurai K, Akahane Y, Sugai Y, et al. Typing hepatitis C virus by polymerase chain reaction with type-specific primers: application to clinical surveys and tracing infectious sources. J Gen Virol 1992;73:673-679.
32. El-Shamy A, Sasayama M, Nagano-Fujii M, Sasase N, Imoto S, Kim SR, et al. Prediction of efficient virological response to pegylated interferon/ribavirin combination therapy by NS5A sequences of hepatitis C virus and anti-NS5A antibodies in pre-treatment sera. Microbiol Immunol 2007;51:471-482.
33. Ogata S, Nagano-Fujii M, Ku Y, Yoon S, Hotta H. Comparative sequence analysis of the core protein and its frameshift product, the F protein, of hepatitis C virus subtype 1b strains obtained from patients with and without hepatocellular carcinoma. J Clin Microbiol 2002;40:3625-3630.
34. Ogata S, Florese RH, Nagano-Fujii M, Hidajat R, Deng L, Ku Y, et al. Identification of hepatitis C virus (HCV) subtype 1b strains that are highly, or only weakly, associated with hepatocellular carcinoma on the basis of the secondary structure of an amino-terminal portion of the HCV NS3 protein. J Clin Microbiol 2003;41:2835-2841.
35. Kato N, Hijikata M, Ootsuyama Y, Nakagawa M, Ohkoshi S, Sugimura T, et al. Molecular cloning of the human hepatitis C virus genome from Japanese patients with non-A, non-B hepatitis. Proc Natl Acad Sci U S A 1990;87:9524-9528.
36. Delhem N, Sabile A, Gajardo R, Podevin P, Abadie A, Blaton MA, et al. Activation of the interferon-inducible protein kinase PKR by hepatocellular carcinoma derived-hepatitis C virus core protein. Oncogene 2001;20:5836-5845.
37. Love RA, Parge HE, Wickersham JA, Hostomsky Z, Habuka N, Moomaw EW, et al. The crystal structure of hepatitis C virus NS3 proteinase reveals a trypsin-like fold and a structural zinc binding site. Cell 1996;87:331-342.
38. Saiz JC, Lopez-Labrador FX, Ampurdanes S, Dopazo J, Forns X, Sanchez-Tapias JM, et al. The prognostic relevance of the nonstructural 5A gene interferon sensitivity determining region is different in infections with genotype 1b and 3a isolates of hepatitis C virus. J Infect Dis 1998;177:839-847.
39. Sarrazin C, Berg T, Lee JH, Teuber G, Dietrich CF, Roth WK, et al. Improved correlation between multiple mutations within the NS5A region and virological response in European patients chronically infected with hepatitis C virus type 1b undergoing combination therapy. J Hepatol 1999;30:1004-1013.

Journal of Virology

# Ifit1 Inhibits Japanese Encephalitis Virus Replication through Binding to 5′ Capped 2′-O Unmethylated RNA

**Taishi Kimura, Hiroshi Katoh, Hisako Kayama, Hiroyuki Saiga, Megumi Okuyama, Toru Okamoto, Eiji Umemoto, Yoshiharu Matsuura, Masahiro Yamamoto and Kiyoshi Takeda**

***J. Virol.*** **2013, 87(18):9997. DOI: 10.1128/JVI.00883-13.**
**Published Ahead of Print 3 July 2013.**

JVI
Journals.ASM.org

# Ifit1 Inhibits Japanese Encephalitis Virus Replication through Binding to 5′ Capped 2′-O Unmethylated RNA

Taishi Kimura,[a,b] Hiroshi Katoh,[d] Hisako Kayama,[a,b,f] Hiroyuki Saiga,[a] Megumi Okuyama,[a] Toru Okamoto,[d] Eiji Umemoto,[a,b,f] Yoshiharu Matsuura,[d] Masahiro Yamamoto,[c,e] Kiyoshi Takeda[a,b,f]

Department of Microbiology and Immunology, Graduate School of Medicine,[a] Laboratory of Mucosal Immunology,[b] and Laboratory of Immunoparasitology,[c] WPI Immunology Frontier Research Center, Osaka University, Osaka, Japan; Department of Molecular Virology[d] and Department of Immunoparasitology,[e] Research Institute for Microbial Diseases, Osaka University, Osaka, Japan; Core Research for Evolutional Science and Technology, Japan Science and Technology Agency, Saitama, Japan[f]

**The interferon-inducible protein with tetratricopeptide (IFIT) family proteins inhibit replication of some viruses by recognizing several types of RNAs, including 5′-triphosphate RNA and 5′ capped 2′-O unmethylated mRNA. However, it remains unclear how IFITs inhibit replication of some viruses through recognition of RNA. Here, we analyzed the mechanisms by which Ifit1 exerts antiviral responses. Replication of a Japanese encephalitis virus (JEV) 2′-O methyltransferase (MTase) mutant was markedly enhanced in mouse embryonic fibroblasts and macrophages lacking Ifit1. Ifit1 bound 5′-triphosphate RNA but more preferentially associated with 5′ capped 2′-O unmethylated mRNA. Ifit1 inhibited the translation of mRNA and thereby restricted the replication of JEV mutated in 2′-O MTase. Thus, Ifit1 inhibits replication of MTase-defective JEV by inhibiting mRNA translation through direct binding to mRNA 5′ structures.**

mRNA has a 5′ cap structure, in which the N-7 position of the guanosine residue is methylated. The 5′ cap structure is known to be responsible for the stability and efficient translation of mRNA (1, 2). In higher eukaryotes, the first one or two 5′ nucleotides are additionally methylated at the ribose 2′-O position by distinct host nuclear 2′-O methyltransferases (MTases) (3, 4). However, the functional role of 2′-O methylation (2′-O Me) remains poorly understood. Several viruses that replicate in the cytoplasm possess their own mRNA capping machineries (5–10). For positive-stranded flaviviruses, nonstructural protein 3 (NS3) acts as an RNA 5′-triphosphatase and NS5 possesses both N-7 and 2′-O MTase activities (8, 11, 12). Recent studies have revealed that 2′-O methylation of the mRNA 5′ cap in these viruses is important for evasion from the host innate immune responses (13–15). However, the 2′-O MTase activity has been shown to be absent from several paramyxoviruses, such as Newcastle disease virus (NDV) and respiratory syncytial virus (RSV) (16, 17).

Type I interferons (IFNs) induce the expression of a large number of antiviral genes through a Janus kinase/signal transducer and activator of transcription (JAK/STAT) pathway (18, 19). Among the IFN-inducible genes, the IFN-inducible protein with tetratricopeptide (IFIT) genes comprise a large family with three (*Ifit1*, *Ifit2*, and *Ifit3*) and four (*IFIT1*, *IFIT2*, *IFIT3*, and *IFIT5*) members in mice and humans, respectively. The murine and human genes are clustered in loci on chromosomes 19C1 and 10q23, respectively (20). IFIT family proteins reportedly associate with several host proteins to exert various cellular functions (21, 22). For example, human IFIT1/IFIT2 and murine Ifit1/Ifit2 bind to eukaryotic translational initiation factor 3 (eIF3) subunits to inhibit translation (23–26). IFIT1 has been suggested to interact with STING/MITA to negatively regulate IRF3 activation (27), whereas IFIT3 may bind TBK1 to enhance type I IFN production and with JAB1 to inhibit leukemia cell growth (28, 29).

In addition to binding host factors, IFIT proteins have functional effects by interacting directly with products of viruses. Human IFIT1 interacts with the human papillomavirus E1 protein and human IFIT2 interacts with the AU-rich RNA of NDV to exert antiviral effects (30, 31). Direct binding of IFIT proteins to virus RNA has also been demonstrated in several recent studies. IFIT1 and IFIT5 bind to the 5′-triphosphate (5′-PPP) RNA that is present in the genomes of viruses (32, 33). Structural studies of human IFIT2 and human IFIT5 identified an RNA-binding site and defined the structural basis of a complex with 5′-PPP RNA (31, 33). However, these structural studies did not explain how IFIT binds to or restricts virus RNA that has a 5′ cap but lacks methylation at the 2′-O position (13–15). Thus, it remains unclear how IFITs mediate antiviral activities against viruses that have a 5′ cap but lack 2′-O MTase activity.

In this study, we analyzed the mechanisms by which murine Ifit1 exerts the host defense against a flavivirus lacking 2′-O MTase activity. Ifit1 was found to preferentially interact with 5′ capped mRNA without 2′-O methylation and inhibit its translation. Thus, Ifit1 participates in antiviral responses targeting 5′ capped mRNA without 2′-O methylation.

## MATERIALS AND METHODS

**Mice.** All animal experiments were conducted in accordance with the guidelines of the Animal Care and Use Committee of the Graduate School of Medicine, Osaka University. The gene-targeting strategies for generating *Ifit1*-knockout (*Ifit1*$^{-/-}$) mice were described previously (34). The *Ifit1*-targeting vector was designed to replace a 1.8-kb fragment encoding the exon of *Ifit1* with a neomycin resistance gene cassette (Neo). A short arm and a long arm of the homology region from the v6.5 embryonic stem (ES) cell genome were amplified by PCR. A herpes simplex virus (HSV) thymidine kinase (tk) gene was inserted into the 3′ end of the vector. After the *Ifit1*-targeting vector was electroporated into ES cells, G418 and ganciclovir doubly resistant clones were selected and screened by PCR and

Received 2 April 2013 Accepted 26 June 2013
Published ahead of print 3 July 2013
Address correspondence to Kiyoshi Takeda, ktakeda@ongene.med.osaka-u.ac.jp.

doi:10.1128/JVI.00883-13

Southern blot analysis. An ES cell clone correctly targeting *Ifit1* was microinjected into C57BL/6 mouse blastocysts. Chimeric mice were mated with female C57BL/6 mice, and heterozygous F1 progenies were intercrossed to obtain $Ifit1^{-/-}$ mice.

**Cells.** HEK293T cells, Vero cells, and mouse embryonic fibroblasts (MEFs) were maintained in Dulbecco's modified Eagle's medium (Nakalai Tesque) supplemented with 10% fetal bovine serum (JRH Bioscience), 100 U/ml penicillin, and 100 μg/ml streptomycin (Gibco). MEFs were prepared from wild-type (WT) and $Ifit1^{-/-}$ day 14.5 embryos and immortalized by introduction of a plasmid encoding the simian virus 40 large T antigen. MEFs stably expressing Ifit1 were established by the previously described method with some modifications (34). In short, full-length cDNA of *Ifit1* was cloned into pMRX-puro (pMRX/*Ifit1*). Retrovirus was produced by introduction of pMRX/*Ifit1* into Plat-E packaging cells (35). MEFs were infected with the retrovirus, cultured in the presence of 1 μg/ml of puromycin (Sigma) for 5 days, and harvested for subsequent studies. To isolate peritoneal macrophages, mice were intraperitoneally injected with 5 ml of 4% thioglycolate medium (Sigma), and peritoneal exudative cells were isolated from the peritoneal cavity at 3 days postinjection. The cells were incubated for 2 h and then washed three times with Hanks' balanced salt solution. The remaining adherent cells were used as peritoneal macrophages in the experiments.

**Viruses.** Japanese encephalitis virus (JEV) strain AT31 (36) was used for the experiments. An NS5 K61A mutation of JEV was introduced into pMWATG1 (37) by PCR-based mutagenesis with the primers 5′-GCGAGGCTCAGCAGCTCTCCGTTGGCTCG-3′ and 5′-CGAGCCAACGGAGAGCTGCTGAGCCTCGC-3′ (the mutagenesis site is underlined) and verified by DNA sequencing. A recombinant virus, the JEV K61A mutant, was generated from pMWJEATG1/JEV K61A as previously described (36). MEFs or macrophages were infected with JEV at specified multiplicities of infection (MOIs). The virus yields in the culture supernatants were titrated by focus-forming assays on Vero cells and expressed as the number of focus-forming units (FFU), as previously described (38). The virus RNA accumulations in the JEV-infected cells were determined by real-time reverse transcription-PCR (RT-PCR) with primers targeting JEV NS5, normalized to the level of host GAPDH (glyceraldehyde-3-phosphate dehydrogenase), and expressed as the fold change in $Ifit1^{-/-}$ cells versus wild-type cells (value for wild type = 1).

**Preparation of RNA.** The 5′-terminal 200 nucleotides of the JEV genome were amplified by PCR using pMWATG1 (37) with the primers 5′-TAATACGACTCACTATTAGAAGTTTATCT-3′ (the T7 class II promoter sequence is underlined) and 5′-CATTACTACCCTCTTCACTCCCACTAGTGG-3′, and the luciferase reporter gene (*luc2*) was amplified using pGL4.14 (Promega) with the primers 5′-TAATACGACTCACTATAGGCCACCATGGAAGATGCCAAAAA-3′ (the T7 class III promoter sequence is underlined) and 5′-TACCACATTTGTAGAGGTTTTACTTGCTTT-3′. Subsequently, the PCR products were *in vitro* transcribed under the control of the T7 promoter with MEGAScript (Ambion). Biotin-labeled RNA was prepared by *in vitro* transcription in the presence of biotin-labeled UTP (PerkinElmer). Capped RNA substrates were produced with a ScriptCap 7-methylguanosine (m7G) capping system (Epicentre) in the presence (5′ cap positive [5′ cap$^+$]/2′-O Me positive [2′-O Me$^+$]) or absence (5′ cap$^+$/2′-O Me negative [2′-O Me$^-$]) of a ScriptCap vaccinia virus 2′-O MTase (Epicentre). $^{32}$P-labeled m7GpppA-RNA substrate was prepared with a ScriptCap m7G capping system in the presence of $^{32}$P-labeled GTP. A 5′ OH-RNA substrate was produced by incubating *in vitro*-transcribed RNA with calf intestinal alkaline phosphatase (CIAP) for 3 h at 37°C. All RNA substrates were purified with an RNeasy minikit (Qiagen) and stored at −80°C until use.

**Real-time RT-PCR.** Total RNA was isolated with the TRIzol reagent (Invitrogen), and 1 to 2 μg of RNA was reverse transcribed using Moloney murine leukemia virus reverse transcriptase (Promega) and random primers (Toyobo) after treatment with RQ1 DNase I (Promega). Real-time RT-PCR was performed in an ABI 7300 apparatus (Applied Biosystems) using a GoTaq real-time PCR system (Promega). All values were normalized by the expression of the GAPDH gene. The following primer sets were used: for the JEV NS5 gene, 5′-AACGCACATTACGCGTCCTAGAGATGA-3′ and 5′-CTAACCCAATACATCTCGTGATTGGAGTT-3′; for *Ifnb*, 5′-GGAGATGACGGAGAAGATGC-3′ and 5′-CCCAGTGCTGGAGAAATTGT-3′; for *luc2*, 5′-CCATTCTACCCACTCGAAGACG-3′ and 5′-CGTAGGTAATGTCCACCTCGA-3′; and for the GAPDH gene, 5′-CCTCGTCCCGTAGACAAAATG-3′ and 5′-TCTCCACTTTGCCACTGCAA-3′.

**Recombinant proteins.** Wild-type and K61A mutant JEV N-terminal NS5 (MTase domain) cDNAs were obtained by PCR using pMWATG1 with the primers 5′-GGATCCGGAAGGCCTGGGGGCAGGACGCTA-3′ and 5′-CTCGAGATGCTCAGGGTCTTTGTGCCACGT-3′. Full-length murine *Ifit1* cDNA and JEV MTase cDNA were inserted into pET-15b and pGEX-6P, respectively. pET/*Ifit1* and pGEX/JEV MTases were transformed into the *Escherichia coli* BL21(DE3) strain. Expression of the Ifit1 and JEV NS5 proteins was induced by addition of 0.5 mM isopropyl-1-thio-β-D-galactopyranoside (IPTG), and the expressed Ifit1 and JEV MTase proteins were purified using $Ni^{2+}$-affinity chromatography (Novagen) and glutathione-Sepharose 4B (Amersham Biosciences), respectively, according to each manufacturer's instructions. The purified protein was desalted and concentrated using an Amicon Ultra centrifugal filter unit (Millipore) and stored at −80°C until use.

***In vitro* MTase activity assay.** The MTase reaction was performed in a 20-μl reaction mixture of 50 mM Tris-HCl (pH 8.0), 6 mM KCl, 1.25 mM $MgCl_2$, and 0.5 mM *S*-adenosylmethionine (AdoMet) containing 10 nmol of $^{32}$P-labeled m7GpppA-RNA substrate (JEV 5′-terminal 200 nucleotides) and 30 pmol of JEV MTase or 80 units of vaccinia virus 2′-O MTase (Epicentre) for 3 h at 37°C. The RNA was purified by passage through a postreaction cleanup column (Sigma) and digested with 10 U of nuclease P1 (Wako) in 50 mM sodium acetate overnight at 37°C. The samples were analyzed on thin-layer chromatography polyethyleneimine (PEI)-cellulose plates developed with 0.3 M ammonium sulfate.

**RNA EMSAs.** RNA electrophoretic mobility shift assays (EMSAs) were performed using a LightShift chemiluminescent RNA EMSA kit (Thermo Scientific) according to the manufacturer's instructions. Briefly, 0 to 20 pmol of recombinant murine Ifit1 and 2.5 pmol of *in vitro*-transcribed and biotin-labeled RNA were coincubated for 30 min at room temperature in RNA EMSA binding buffer (10 mM HEPES, pH 7.3, 20 mM KCl, 1 mM $MgCl_2$, 1 mM dithiothreitol, 0.1 μg/μl of yeast tRNA, 2% glycerol). The resulting Ifit1/RNA complexes were electrophoresed in a 7.5% native polyacrylamide gel. The separated RNAs were transferred to a positively charged nylon membrane and cross-linked at 120 mJ/cm$^2$ and an absorbance of 254 nm. The membrane was incubated with stabilized streptavidin-horseradish peroxidase conjugate (1:300 dilution; a component of the EMSA kit), and the bound stable peroxide was detected with luminol/enhancer solution (another component of the EMSA kit). The gel-shift band intensities were quantified using ImageJ software (National Institutes of Health).

**RNA pulldown assay.** For RNA pulldown assays, an expression vector for hemagglutinin (HA)-tagged murine full-length Ifit1 was transfected into HEK293T cells using Lipofectamine 2000 (Invitrogen). The *Ifit1*-transfected cells were lysed in RNA-binding buffer (10 mM HEPES, pH 7.3, 500 mM KCl, 1 mM EDTA, 2 mM $MgCl_2$, 0.1% NP-40, 0.1 μg/μl of yeast tRNA (Ambion), 1 U/ml of RNase inhibitor [Toyobo]), and the lysate (200 μg) was coincubated with 25 pmol of biotin-labeled RNA and streptavidin-agarose (Invitrogen) in RNA-binding buffer for 30 min at room temperature. The binding complexes were washed five times with RNA-binding buffer, followed by SDS-PAGE and immunoblotting with an anti-HA probe (F-7) antibody (Santa Cruz Biotechnology). The intensity of the detected Ifit1 band was quantified using ImageJ software (National Institutes of Health).

**RNA immunoprecipitation.** RNA immunoprecipitation was performed as described previously (38) with slight modifications. MEFs ($2 \times 10^5$) stably expressing Flag-tagged Ifit1 were infected with JEV at an MOI of 1.0 and cultured for 24 h. The cells were then lysed in 500 μl of RNA

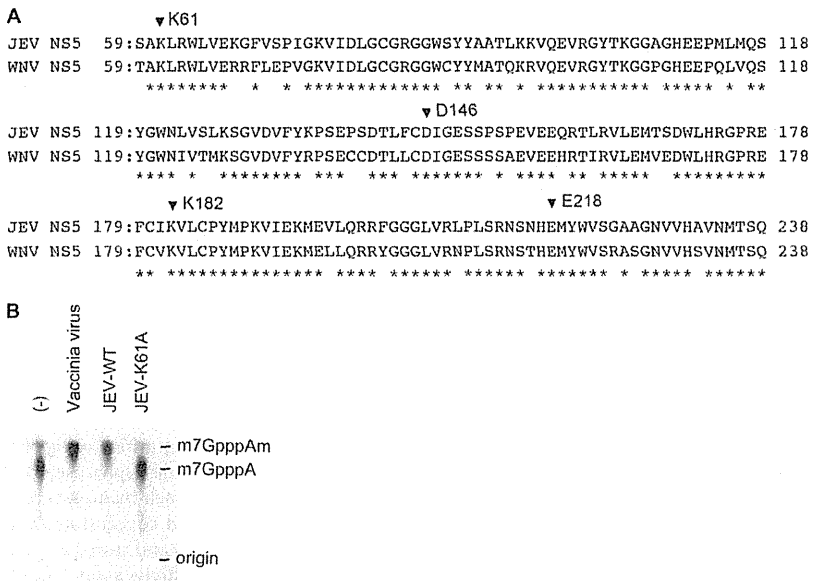


FIG 1 Generation of an MTase-defective JEV mutant. (A) Sequence homology between NS5 proteins of JEV (AT31 strain, GenBank accession number AB196926) and WNV (00-3356 strain, GenBank accession number EF530047). Arrowheads, MTase catalytic K-D-K-E tetrad; *, consensus sequences between the two proteins. (B) 2′-O MTase activity of JEV WT and JEV K61A mutant recombinant NS5 proteins by thin-layer chromatography assays. The substrate m7GpppA-RNA ($^{32}$P-labeled JEV 5′-terminal 200 nucleotides) was methylated *in vitro* with the respective recombinant NS5 proteins or vaccinia virus 2′-O MTase, digested with P1 nuclease, and developed on PEI-cellulose plates. The positions of 2′-O methylated (m7GpppAm) and unmethylated (m7GpppA) RNA are indicated. Data are representative of four independent experiments.

buffer (10 mM HEPES, pH 7.3, 500 mM KCl, 1 mM EDTA, 2 mM $MgCl_2$, 0.1% NP-40, 0.1 μg/μl of yeast tRNA (Ambion), 1 U/ml of RNase inhibitor [Toyobo], 1 tablet/10 ml of Complete mini-protease inhibitor cocktail [Roche]). After centrifugation at 15,000 rpm for 20 min at 4°C, 50-μl aliquots of the supernatants were recovered as input samples and the remaining supernatants were precleared with 30 μl of 50% protein G-conjugated Sepharose and 1 μg of mouse normal IgG for 1 h. After centrifugation of the beads, the supernatants were immunoprecipitated with 1 μg of mouse normal IgG or anti-Flag M2 antibody (Santa Cruz Biotechnology) and 30 μl of 50% protein G-conjugated Sepharose. The beads were washed five times with RNA buffer without yeast tRNA, and RNA was isolated from the precipitants and input samples with the TRIzol reagent. The RNA was reverse transcribed as described above and subjected to the first round of PCR with JEV NS1-specific primers 5′-TCTG TCACTAGACTGGAGCA-3′ and 5′-CCAGAAACATCACCAGAAGG-3′. The PCR products were then analyzed by quantitative PCR with nested primers 5′-GAGCACTGACGAGTGTGATG-3′ and 5′-AGCGACTCTC AATCCAGTAC-3′. All values were normalized by the values for the input samples (indicated as percent input).

**Cellular translational reporter assay.** MEFs ($2 \times 10^5$) were pretreated with 1,000 U/ml of universal type I interferon (PBL Biomedical Laboratories) for 6 h. Three types of 5′ modified luciferase mRNAs (2 μg of 5′-PPP, 5′ cap$^+$/2′-O Me$^-$, and 5′ cap$^+$/2′-O Me$^+$) were transiently transfected into MEFs using the Lipofectamine 2000 reagent (Invitrogen) according to the manufacturer's instructions. At 6 h after the transfection, RNA was isolated and analyzed for the quantity of the luciferase mRNAs (*luc2*). The luciferase activities of whole-cell lysates were measured using a dual-luciferase reporter assay system (Promega). The numbers of relative light units (RLU) were normalized by the concentrations of proteins determined by use of a bicinchoninic acid protein assay kit (Thermo Scientific).

**Statistical analysis.** Statistical analyses were conducted on each independent data set. An unpaired Student's *t* test was used to determine the statistical significance of differences in the experimental data. *P* values of $<0.05$ were considered to indicate statistical significance.

## RESULTS

***Ifit1*$^{-/-}$ cells fail to restrict the replication of a mutant JEV lacking 2′-O MTase activity.** Previous analysis of the flavivirus West Nile virus (WNV) 2′-O MTase revealed residues in NS5 (K61, D146, K182, and E218) that were essential for its biochemical activity (8). A WNV mutant (E218A) lacking 2′-O MTase activity was attenuated in mouse MEFs and macrophages but showed enhanced replication in *Ifit1*$^{-/-}$ cells (13, 15). As NS5 is a highly conserved protein in flaviviruses, the four residues integral to the 2′-O MTase activity are identical in WNV and JEV (Fig. 1A). Replacement of lysine 61 by alanine in the JEV NS5 MTase domain (JEV K61A) abolished the JEV 2′-O MTase activity *in vitro* (Fig. 1B). We generated *Ifit1*$^{-/-}$ mice (Fig. 2A to C) and infected MEFs with JEV WT and JEV K61A strains (Fig. 3A). The JEV WT replicated equivalently in wild-type and *Ifit1*$^{-/-}$ MEFs. In comparison, the production of the JEV K61A mutant was decreased in wild-type MEFs, suggesting that 2′-O MTase activity is required for JEV replication. Consistent with this and analogous studies with an WNV E218A strain (13), replication of the JEV K61A strain was enhanced (approximately 173-fold increased at 4 days postinfection; $P < 0.05$) in *Ifit1*$^{-/-}$ MEFs compared with wild-type MEFs. We also infected peritoneal macrophages with JEV WT and JEV K61A strains (Fig. 3B). Similar to the results obtained with MEFs, replication of the JEV WT was similarly observed in wild-type and *Ifit1*$^{-/-}$ macrophages. However, replication of the JEV K61A mutant was severely decreased in wild-type but not *Ifit1*$^{-/-}$ macrophages, and the virus was not detected at 4 days postinfection in wild-type cells. For further confirmation, we analyzed virus RNA accumulation at 4 days postinfection (Fig. 3C and D). Whereas RNA levels of JEV WT were similar in wild-type and *Ifit1*$^{-/-}$ MEFs, those of the JEV K61A mutant were markedly

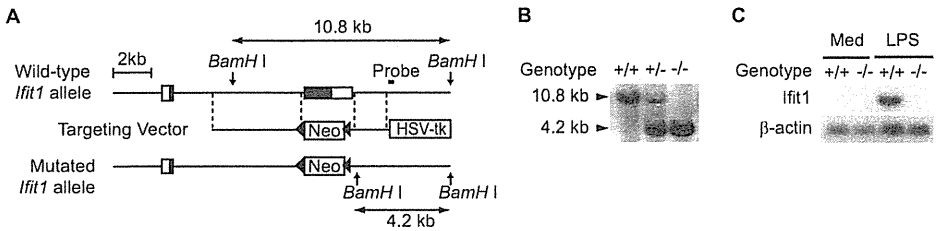


FIG 2 Generation of *Ifit1*$^{-/-}$ mice. (A) Schematic representation of the *Ifit1* gene-targeting strategies. Solid boxes, coding regions of the *Ifit1* gene; open boxes, untranslated regions; Neo and HSV tk, a neomycin-resistance gene cassette and a herpes simplex virus thymidine kinase gene, respectively. The positions of the probe and restriction enzyme site for Southern blotting are shown. (B) Genomic DNA was isolated from the tails of wild-type (+/+), heterozygous (+/-), and homozygous (−/−) *Ifit1* mutant mice. A Southern blot analysis performed after digestion of the genomic DNA with BamHI shows the correct targeting of the locus. (C) Peritoneal exudative macrophages were harvested from wild-type (+/+) or *Ifit1*-deficient (−/−) mice. Total RNA (10 μg) was blotted onto a nylon membrane, and Ifit1 and β-actin mRNA expression was detected by Northern blot analysis with the respective cDNA probes. LPS lanes, cells stimulated with 100 ng/ml of lipopolysaccharide for 4 h to induce endogenous Ifit1 expression; Med lanes, cells treated with medium alone.

higher (approximately 13-fold; $P < 0.05$) in *Ifit1*$^{-/-}$ MEFs than in wild-type MEFs. To further corroborate these findings, we reintroduced the *Ifit1* gene into *Ifit1*$^{-/-}$ MEFs using a retrovirus vector. Replication of the JEV K61A mutant was considerably suppressed (approximately 4-fold; $P < 0.05$) by ectopic Ifit1 expression in *Ifit1*$^{-/-}$ MEFs (Fig. 3E). *Ifnb* was similarly induced in wild-type and *Ifit1*$^{-/-}$ MEFs after infection with the JEV K61A mutant, excluding the possibility that defective type I IFN production is responsible for the high sensitivity to infection with the JEV K61A mutant in *Ifit1*$^{-/-}$ cells (Fig. 3F). Thus, consistent with the findings of previous studies (13, 15), Ifit1 inhibits replication and infection of flavivirus mutants that lack 2′-O MTase activity.

**Ifit1 preferentially binds to virus RNA lacking 2′-O methylation.** Next, we analyzed how Ifit1 recognizes 2′-O MTase mutant

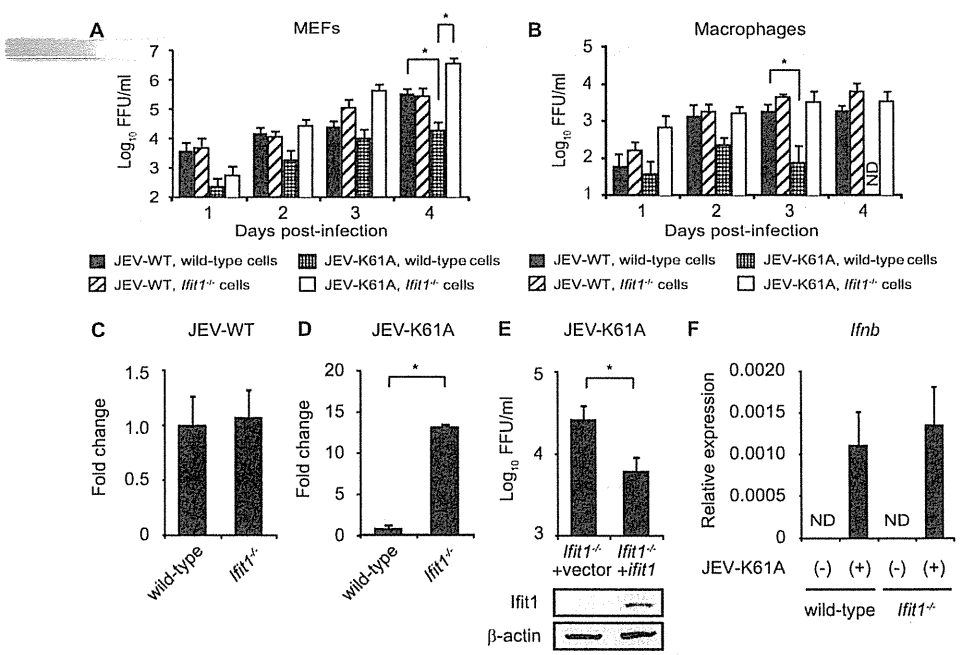


FIG 3 *Ifit1*$^{-/-}$ MEFs and macrophages fail to restrict the replication of the 2′-O MTase mutant JEV. (A, B) Culture supernatants of wild-type and *Ifit1*$^{-/-}$ MEFs (A) and macrophages (B) infected with JEV WT and the JEV K61A mutant (MOIs, 0.1 for MEFs and 0.5 for macrophages) were harvested at the indicated days postinfection. The virus titers in 1-ml supernatant aliquots were determined by focus-forming assays on Vero cells and expressed as the $\log_{10}$ number of FFU/ml. Data are shown as means ± SDs of quadruplicate samples generated from four independent experiments with statistical significance. ND, not detected. *, $P < 0.05$. (C, D) Accumulation of JEV WT (C) and the JEV K61A mutant (D) RNA in wild-type and *Ifit1*$^{-/-}$ MEFs at 4 days postinfection determined by quantitative real-time RT-PCR. JEV NS5 RNA levels were normalized to the level of host GAPDH and are expressed as the fold change in *Ifit1*$^{-/-}$ cells versus wild-type cells (value for wild type = 1). Data are representative of three independent experiments with statistical significance. *, $P < 0.05$. (E) Culture supernatants of vector-transduced (+vector) and Flag-tagged *Ifit1* gene-transduced (+*Ifit1*) *Ifit1*$^{-/-}$ MEFs infected with the JEV K61A mutant (MOI, 0.1) were harvested at 3 days postinfection. The virus titers in 1-ml supernatant aliquots were determined by focus-forming assays on Vero cells and expressed as the $\log_{10}$ number of FFU/ml. Expression of Ifit1 and β-actin determined by immunoblotting with anti-Flag or anti-β-actin antibodies is shown at the bottom. Data are representative of three independent experiments. *, $P < 0.05$. (F) Wild-type and *Ifit1*$^{-/-}$ MEFs were infected with the JEV K61A mutant (MOI, 0.1). At 4 days postinfection, cells were harvested and analyzed for *Ifnb* expression by quantitative RT-PCR. *Ifnb* RNA levels were expressed relative to those of GAPDH. ND, not detected. Data are shown as means ± SDs and are representative of data from three independent experiments.

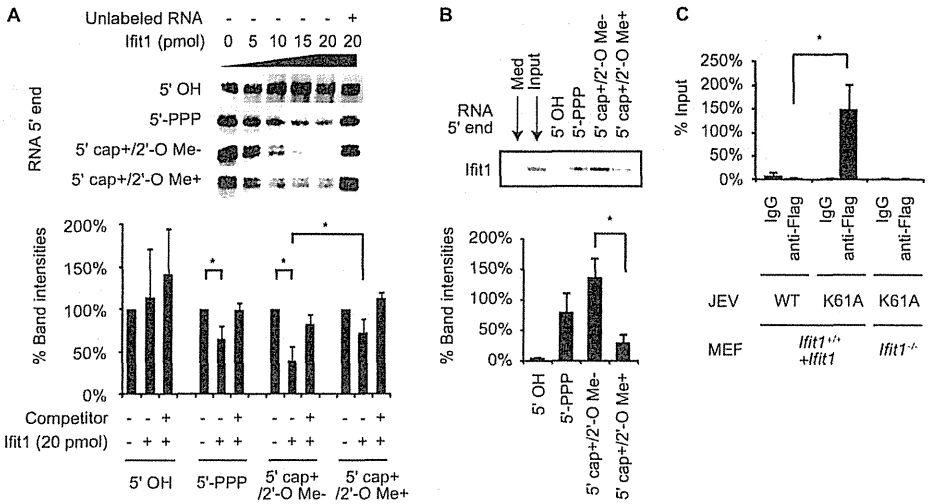


FIG 4 Ifit1 preferentially binds to virus RNA lacking 2′-O methylation. (A) Electrophoretic mobility shift of biotin-labeled RNA (JEV 5′-terminal 200 nucleotides) with recombinant Ifit1. The presence or absence of a 5′ cap and 2′-O Me of the JEV 5′-terminal 200 nucleotides is indicated. Unlabeled 5′-PPP RNA was used as a competitor. The loss of the band indicates binding of RNA and Ifit1 (top). The band intensities (in percent) calculated by ImageJ are shown at the bottom. Data are representative (top) and means ± SDs (bottom) of five independent experiments. *, $P < 0.05$. (B) Lysates from HEK293T cells transfected with HA-tagged Ifit1 were incubated with 2.5 pmol of biotin-labeled RNA. The presence or absence of a 5′ cap and 2′-O Me of the JEV 5′-terminal 200 nucleotides is indicated. 5′ OH RNA was produced by incubating *in vitro*-transcribed RNA with CIAP. RNA was incubated with streptavidin beads, and the precipitates were separated by SDS-PAGE and immunoblotted with an anti-HA antibody (top). Med and Input, samples from whole-cell lysates of empty vector- and *Ifit1*-transfected 293T cells, respectively. The percent band intensities calculated by ImageJ are shown at the bottom. Data are representative (top) and means ± SDs (bottom) of three independent experiments. *, $P < 0.05$. (C) MEFs stably expressing Ifit1 (*Ifit1*$^{+/+}$ + *Ifit1*) or *Ifit1*$^{-/-}$ MEFs were infected with JEV WT or the JEV K61A mutant at an MOI of 1.0. The cells were harvested after 24 h, and JEV RNA/Ifit1-binding complexes were immunoprecipitated with a mouse anti-Flag antibody or mouse IgG. The immunoprecipitated RNA was analyzed by nested RT-PCR using primers that detect the JEV NS1 gene. Each value was normalized by the value for the input (indicated in percent). Data are means ± SDs of three independent experiments. *, $P < 0.05$.

viruses. While recombinant IFIT1 reportedly binds to 5′-PPP RNA (32), the mRNA of the JEV K61A mutant has a 5′ m7G cap but lacks 2′-O methylation (5′ cap$^+$/2′-O Me$^-$). We examined whether Ifit1 can also interact directly with 5′ cap$^+$/2′-O Me$^-$ RNA using electrophoretic mobility shift assays. Consistent with a previous report (32), bands of 5′-PPP RNA but not RNA lacking phosphate at the 5′ end (5′ OH) were diminished after addition of recombinant Ifit1 (Fig. 4A). Furthermore, Ifit1 blocked the electrophoretic mobility of the 5′ cap$^+$/2′-O Me$^-$ RNA. However, this effect was rescued by exogenous addition *in vitro* of 2′-O methylation (5′ cap$^+$/2′-O Me$^+$). The efficient binding of Ifit1 to 5′ cap$^+$/2′-O Me$^-$ RNA was corroborated by RNA pulldown assays (Fig. 4B). HA-tagged Ifit1 was expressed in HEK293T cells, and cell lysates were incubated with biotin-labeled *in vitro*-transcribed RNA and streptavidin-agarose. Then, binding complexes of Ifit1/RNA were analyzed by Western blotting. While Ifit1 was not pulled down with 5′ OH RNA, modest binding of Ifit1 to 5′-PPP RNA and 5′ cap$^+$/2′-O Me$^+$ RNA was observed. In comparison, the strongest Ifit1 protein signal was observed with 5′ cap$^+$/2′-O Me$^-$ RNA. These findings suggest that Ifit1 preferentially binds to 5′ capped RNA lacking 2′-O methylation.

To confirm independently that Ifit1 interacts with 5′ capped RNA lacking 2′-O methylation, we performed RNA immunoprecipitation assays using cell lysates from JEV-infected MEFs that ectopically expressed a Flag-tagged Ifit1. After immunoprecipitation with an anti-Flag antibody, the JEV mRNA was measured by nested RT-PCR analysis (Fig. 4C). JEV RNA was only marginally detected in lysates precipitated with control IgG and lysates of *Ifit1*$^{-/-}$ MEFs infected with the JEV K61A mutant, indicating the specificity of Ifit1 binding in the assay. Virus RNA in JEV K61A mutant-infected MEFs was detected at a level over 37-fold higher than that in JEV WT-infected MEFs. Taken together, these findings suggest that Ifit1 directly interacts with virus mRNA lacking 2′-O methylation.

**Ifit1 selectively inhibits translation of 5′ capped 2′-O unmethylated mRNA.** To examine the mechanism by which Ifit1 exerts an antiviral effect by associating with mRNA lacking 2′-O methylation, we used a luciferase translational reporter assay. Luciferase RNAs with different 5′ structures were transfected into type I IFN-primed MEFs, and total RNA and cell lysates were harvested 6 h later. Importantly, the levels of luciferase RNAs in wild-type and *Ifit1*$^{-/-}$ cells were unaffected by any of the 5′ modifications (Fig. 5A). We then analyzed the translational efficiency of the transfected RNAs by measuring the luciferase activity (Fig. 5B). As expected (1), uncapped 5′-PPP luciferase mRNA was not translated in either wild-type or *Ifit1*$^{-/-}$ MEFs. Capping of the mRNA (5′ cap$^+$/2′-O Me$^-$) increased translation in wild-type cells, although the levels were profoundly lower ($P < 0.05$) than those in *Ifit1*$^{-/-}$ cells. In comparison, addition of 2′-O methylation to the 5′ cap (5′ cap$^+$/2′-O Me$^+$) *in vitro* resulted in similar levels of translation in wild-type and *Ifit1*$^{-/-}$ MEFs. Even in MEFs that were not treated with type I IFN, similar patterns of luciferase activity were observed (Fig. 5C), indicating that slightly expressed Ifit1 might contribute to the inhibition. Taken together, our data establish that Ifit1 preferentially binds to 5′ capped mRNA lacking 2′-O methylation and inhibits its translation.

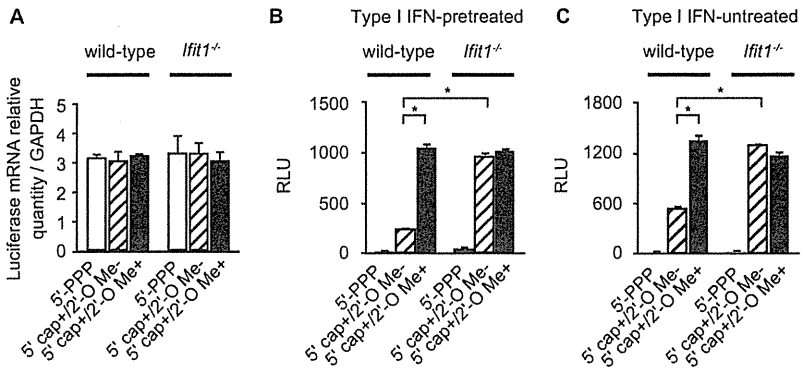


FIG 5 Ifit1 selectively inhibits the translation of mRNA lacking 2′-O methylation. (A) The luciferase RNA amounts at 6 h after RNA transfection were determined by quantitative real-time RT-PCR. The relative luciferase mRNA amounts, calculated as the amount of each transfected mRNA (*luc2*) divided by the level of GAPDH mRNA expression, are shown. The presence or absence of a 5′ cap and 2′-O Me of the introduced luciferase RNA is indicated. Data are shown as means ± SDs and are representative of three independent experiments. (B, C) Wild-type and *Ifit1*$^{-/-}$ MEFs pretreated with type I IFN (B) or untreated (C) were transiently transfected with luciferase mRNA. Luciferase activities were measured at 6 h after the transfection and are shown as relative light units (RLU). The presence or absence of a 5′ cap and 2′-O Me of the introduced luciferase RNA is indicated. Data are shown as means ± SDs of triplicate samples of the representative results. Similar results were obtained in three independent experiments. *, $P < 0.05$.

## DISCUSSION

In this study, we investigated the mechanisms by which Ifit1 recognizes RNA of JEV lacking 2′-O MTase activity. Ifit1 inhibited the translation of mRNA through association with mRNA lacking 2′-O methylation.

To analyze the role of Ifit1 in 5′ cap structure-dependent antiviral responses, we generated a JEV MTase mutant. The K61, D146, K182, and E218 residues have all been shown to be essential for the MTase activity of the NS5 protein and replication of WNV (8, 11). While a WNV E218A mutant was previously used for analysis of Ifit1-mediated antiviral responses (13), in our assays, the corresponding JEV E218A mutant was severely impaired in replication in Vero cells and rapidly reverted to the wild type during cell culture, preventing its use (data not shown). A similar phenotype was observed with the WNV D146A 2′-O methylation mutant (11). However, unlike our results, it has recently been reported that a JEV E218A mutant is stable in Vero cells (39). This would be due to the different strains used in the two studies. Thus, mutation of residues that are essential for the 2′-O MTase activity of a flavivirus NS5 protein can differentially impact replication of JEV and WNV even in cells lacking type I IFN responses and IFIT1 expression.

Previous *in vitro* studies indicated that IFIT family proteins bind to several types of RNA, including 5′-PPP RNA and AU-rich double-stranded RNA (31, 32). Indeed, an analysis of the IFIT2 crystal structure indicated the presence of a positively charged RNA-binding channel (31), findings which were supported by the X-ray crystallographic structure of complexes of 5′-PPP RNA with human IFIT5 (33, 40). We also observed that Ifit1 could bind to 5′-PPP RNA. However, our biochemical analysis showed that Ifit1 bound strongly to 5′ capped RNA lacking 2′-O methylation and addition of 2′-O methylation weakened the binding of Ifit1 to the RNA. Since mRNAs of virtually all higher eukaryotes are believed to be methylated at the ribose 2′-O position (41), this modification likely serves as a molecular pattern for discriminating self from nonself.

Although it remains unclear how 2′-O methylation reduces Ifit1 binding to RNA, structural changes to the RNA at the 5′ terminus after 2′-O methylation could sterically hamper Ifit1 binding. The crystal structure of the 5′-PPP RNA/IFIT5 complex has indicated that the RNA-binding site on human IFIT5 is located in a narrow pocket, thus raising the possibility that 5′ capped and 2′-O methylated RNA cannot fit within an analogous pocket of Ifit1 due to a size limitation (33). Future structural analyses of the binding complex of 5′ capped RNA with Ifit1 will be required to reveal the precise mechanisms by which Ifit1 recognizes 5′ capped RNA lacking 2′-O methylation. Additional studies must also test whether other IFITs preferentially associate with 5′ capped RNA lacking 2′-O methylation.

Ifit1 also has an antiviral activity against several negative-stranded viruses, such as vesicular stomatitis virus (VSV) and parainfluenza virus type 5 (PIV5) (32, 42), whose mRNAs are 2′-O methylated (6, 42). In this regard, Ifit1 is supposed to have an antiviral effect independent of 2′-O methylation. Indeed, IFIT1 is able to bind 5′-PPP genomic RNA (32).

Given the previous and present findings that Ifit1 inhibits mRNA translation (23–26), our data are most consistent with a model in which Ifit1 restricts replication of viruses with 5′ capped RNA lacking 2′-O methylation through direct RNA binding and subsequent inhibition of translation. Human IFIT1 and murine Ifit1 were previously reported to interact with eIF3 to interfere with translation (23–26), and replication of hepatitis C virus, whose RNA lacks a 5′ cap, was also impaired by IFIT1 through binding to eIF3 (43). Thus, Ifit1 may associate with both eIF3 and virus mRNA to inhibit translation and infection.

The Ifit family proteins consist of several conserved members. However, Ifit1 and Ifit2 appear to have distinct antiviral activities (44). Thus, the nonredundant and redundant roles of the Ifit family proteins remain to be elucidated. Generation of mice lacking the other members or all of the Ifit family proteins will be useful to reveal the physiological functions.

## ACKNOWLEDGMENTS

We thank M. S. Diamond for fruitful discussions and suggestions, T. Wakita for providing us with the JEV AT31 strain, and T. Kitamura for providing us with Plat-E cells. We also thank Y. Magota for technical assistance, C. Hidaka for excellent secretarial assistance, and members of the K. Takeda laboratory for discussions.

This work was supported by grants from the Ministry of Education, Culture, Sports, Science and Technology, the Japan Science and Technology Agency, and The Osaka Foundation for Promotion of Clinical Immunology.